Phylogenomics and biogeography of the world's thrushes (Aves, *Turdus*): New evidence for a more parsimonious evolutionary history.

Romina Batista[1,2,3*], Urban Olsson[3,4], Tobias Andermann[3,4], Alexandre Aleixo[5], Camila Cherem Ribas[6, †], Alexandre Antonelli[3,4,7 †]

[1] Programa de Pós-Graduação em Genética, Conservação e Biologia Evolutiva, PPG GCBEv - Instituto Nacional de Pesquisas da Amazônia- INPA Campus II. Av. André Araújo, 2936 – Petrópolis - CEP 69067-375 - Manaus - AM, Brazil

[2] Coordenação de Zoologia, Laboratório de Biologia Molecular, Museu Paraense Emílio Goeldi, CEP 66077-830, Belém - PA, Brazil

[3] Gothenburg Global Biodiversity Centre, Box 461, SE-405 30 Gothenburg, Sweden

[4] Department of Biological and Environmental Sciences, University of Gothenburg, SE-413 19 Gothenburg, Sweden

[5] Finnish Museum of Natural History, University of Helsinki, P.O. Box 17, 00014, Helsinki, Finland

[6] Instituto Nacional de Pesquisas da Amazônia, INPA Campus II. Av. André Araújo 2936, CEP 69060-000, Manaus-AM, Brazil

[7] Royal Botanic Gardens, Kew, Richmond, Surrey, TW9 3AE, U.K.

[†] Joint senior authors

*E-mail: rominassbatista@gmail.com

Abstract

To elucidate the relationships and spatial range evolution across the world of the bird genus *Turdus* (Aves), we produced a large genomic dataset comprising ca. 2 million nucleotides for ca. 100 samples representing 53 species, including over 2,000 loci. We estimated time-calibrated maximum likelihood and multispecies coalescent phylogenies and carried out biogeographic analyses. Our results indicate that there have been considerably fewer trans-oceanic dispersals within the genus *Turdus* than previously suggested, such that the Palaearctic clade did not originate in America and the African clade was not involved in the colonization of the Americas. Instead, our findings suggest that dispersal from the Western Palaearctic via the Antilles to the Neotropics might have occurred in a single event, giving rise to the rich Neotropical diversity of *Turdus* observed today, with no reverse dispersals to the Palaearctic or Africa. Our large multilocus dataset, combined with dense species-level sampling and analysed under probabilistic methods, brings important insights into historical biogeography and systematics, even in a scenario of fast and spatially complex diversification.

Keywords: *Turdus*, dispersal, next-generation sequencing, species radiations.

Introduction

The family Turdidae (Aves, Passeriformes) comprises 21 genera distributed worldwide, where *Turdus* is the most species-rich genus (86 spp. [1]), accounting for half of the family's species diversity. Species in the genus are generally similar in shape, but show large variation in plumage colouration and ecology, exhibiting a variety of colour patterns and inhabiting almost all biomes in the world – including, savannas, alpine areas and both tropical and temperate forests [1]. This genus contains many common and familiar species throughout the world, such as the Blackbird (*Turdus merula*), the American Robin (*Turdus migratorius*) and the Clay-colored Thrush or yigüirro (*Turdus grayi*).

Previous attempts to resolve phylogenetic relationships within *Turdus* have yielded conflicting phylogenetic hypotheses, and, consequently, different biogeographical interpretations [2-4]. One of their main limitations so far has been the reliance on a very limited number of independent genetic markers, making the analyses vulnerable to stochastic effects. Voelker *et al*. [2], using only mitochondrial DNA, recovered four main clades (African, Central America-Caribbean, South American and Eurasian), but their topology lacked nodal support for all but the Eurasian and a South American clade, with the latter also including an African species. Based on their results, the authors suggested including the genera *Platycichla*, *Cichlerminia* and *Nesocichla* within *Turdus*. In another study, Nylander *et al*. [3] analysed a combined data set from mitochondrial and nuclear markers and inferred one Eurasian, three American and three African clades. Their results led those authors to suggest that: i) the apparent non-monophyly of the African taxa might be illusory; ii) several independent dispersal events have taken place from an African source to South America; and iii) that *Platycichla*, *Cichlerminia* and *Nesocichla* should indeed be placed within *Turdus*. Due to the partially conflicting results of these studies, the evolutionary relationships and biogeographical history within *Turdus* remain unresolved.

The phylogenetic uncertainties concern not only relationships and biogeographic history among the major clades in *Turdus*, but also the taxonomic and phylogeographic implications of recently diverged polytypic species and species complexes. Recent phylogeographic studies of species complexes within *Turdus* revealed additional taxonomic complexity at the level previously regarded as intraspecific, indicating that current taxonomy underestimates the true species diversity within the genus [5-8].

In summary, the controversies surrounding the early diversification and biogeography of *Turdus*, the circumscription and relationships among major clades and species, and our insufficient knowledge of intraspecific divergences and species limits, make *Turdus* a prime candidate for testing the utility of phylogenomic approaches for tackling evolutionary questions among and within bird species.

In this study, we address the following questions: 1) Can phylogenomic data confidently delimit major clades within *Turdus* and elucidate the relationships among them? 2) How many trans-Atlantic dispersals happened during the diversification of *Turdus*, leading to its current cosmopolitan distribution? and 3) Has the African continent functioned as a source for intercontinental dispersals? To address these questions, we infer the phylogeny of the genus *Turdus* based on novel and extensive genomic data (ultraconserved elements (UCEs), intragenic and untranslated regions, respectively) and multiple analytical approaches (maximum likelihood, species tree inference, ancestral area reconstructions). To maximize taxonomic sampling, we also compiled and analysed a dataset of sequences of the

mitochondrial marker cytochrome *b* (cyt*b*), for all currently recognized species within the genus [2, 3, 5, 6, 9].

Methods

A full description of the data and methods can be found in the electronic supplementary material (Table S1, S2, S3, S4, Fig. S1). The overall sampling included 115 individuals from 53 species (~62%) of 86 currently recognized species within the genus *Turdus* [1]. We used a UCE probe set developed by Faircloth *et al*. [10], and developed additional specific probes for *Turdus* based on 49 of the loci described in Backström *et al*. [11].

Phylogenomic and divergence time estimates

We performed unpartitioned concatenated maximum likelihood (ML) analyses in RAxML 8.2.9 [12] for two data sets: 1) a matrix including UCEs (two different thresholds of missing data, 75% and 85%); and 2) a matrix including the additional non-UCE loci (intragenic and untranslated regions). We assessed support for the best ML topology by performing 150 nonparametric bootstrap replicates using the autoMRE option in RAxML with the GTR GAMMA site-rate substitution model.

To avoid loci that could bias species tree analyses, we calculated the number of parsimony-informative sites (PIS) for each UCE locus and created a subset of UCE loci having a number of PIS in the upper quartile of the range (every locus with equal or more than 65 PIS). For the additional non-UCE loci, we included all markers recovered. We performed nonparametric bootstrapping by sites for each locus using RAxML with GTR-GAMMA model of site-rate substitution and sorted the bootstrapped gene trees following Seo [13], an approach for estimating phylogeny and calculating bootstrapping using multilocus sequence data in the context of a distance method. To infer the species tree and calculate nodal support from the frequency of splits in trees constructed, we input the results to ASTRAL-II 4.7.8 [14]. We set ASTRAL to run 150 bootstrap replicates of species trees. We also performed a species tree analysis using SVDquartets [15] for the UCE loci, including all loci recovered. By analysing fewer loci for the species tree, we were able to compare the results using different approaches.

To estimate divergence times, we used two late Miocene fossils from Hungary, correlated to the Mammal Neogene zone 13 (MN13) (7.2-4.9 mya). These two fossils were compared to *T. viscivorus, T. pilaris* and *T. torquatus,* and *T. merula* and *T. philomelos*, respectively. We tentatively interpret this as that they represent forms contemporary with the stem node of the main global radiation of thrushes, and use them for setting the minimum age for the clade including *all Turdus species minus T. philomelos and T. viscivorus* (Fig. 3). To fix a maximum age for this same node, we used the minimum age for the split between Regulidae and Certhioidea (17.2 Ma), based on fossil data and assigned in [16] (Fig. 3). As an additional secondary calibration point, we added the split between Muscicapidae and Turdidae, with a confidence interval of 22-13.5 Mya gleaned from [16] (Fig. 3). A UCE ML tree (the topology recovering highest support values overall) was time-calibrated under penalized likelihood using treePL [17]. The rate smoothing parameter was set to 100. The smoothing value was established using the cross-validation parameter available in treePL, we left the cvstart = 1000 (default) and cvstop = 0.1 (default).

Biogeographic analyses

To infer the spatial range evolution for *Turdus*, we used Biogeography with Bayesian (and likelihood) Evolutionary Analysis in R Scripts – BioGeoBEARS, version 0.2.1 [18]. We

used the time-calibrated phylogeny for *Turdus* calculated in treePL and coded each species as present or absent, according to their ranges following del Hoyo [1]. Eight biogeographical areas were defined based on the zoogeographical realms estimated in [19], with adaptations (Fig. 3): 1. Afrotropical (Afr), 2. Western Palaearctic (WP), 3. Eastern Palaearctic (EP); 4. Oriental (O), 5. Nearctic (N), 6. Panamanian (C); 7. Antilles (Ant); 8. South America (SA).

Results

Phylogenetic relationships

Our results using different thresholds of concatenated UCEs datasets (75% and 85%) recovered *Turdus viscivorus* (historical samples GNM8238 and GNM172, from Sweden) and *T. philomelos* (U4329, from Belarus) as incremental sisters to all other *Turdus* species (Fig. 1, Fig. S2 and Fig. S3). In the main clade, all taxa from the Afrotropical Region, including *T. pelios*, previously contentiously placed as part of the South American radiation, form a strongly supported monophyletic radiation (Node A, Fig. 1, Fig. S2), that is sister to a clade composed of all other species. The Palaearctic clade contains *T. iliacus* and *T. merula*, with strong support. In previous studies, these two species have been found in varying phylogenetic positions that suggest different biogeographical histories from other Western Palaearctic species [2,3]. We consider the following cut-offs for bootstrap values: 50-74% weak; 75-84% moderate and >85% as strong support (Fig. S2, Fig. 1).

While support for both the African and the Eurasian clades is strong, support for a monophyletic group [Node D, Fig. 1] in the Americas is weak. The important first splits within this clade are weakly supported, but the topology suggests a first divergence between Antillean taxa (a strongly supported clade including *T. aurantius* from Jamaica, *T. plumbeus schistaceus* from Cuba and *T. plumbeus ardosiacus* from Puerto Rico) and remaining taxa (Fig. 1). The following basal divergences are all between taxa now inhabiting the Nearctic, Panamanian or Antillean regions [19]. Although the divergence pattern is mostly weakly supported, a biogeographical structure may be discernible. A strongly supported clade comprises mainly species found in Central America (*T. rufitorques*, *T. nigrescens*, *T. infuscatus*), but also *T. migratorius*, a species widely distributed in North America. An exclusively Panamanian clade (strongly supported) consists of two subspecies of *T. plebejus* (*rafaelenses* from Nicaragua and *plebejus* from Panama). A large and strongly supported monophyletic Neotropical radiation (node E; Fig. 1) includes the early (but poorly supported) sequential divergence of two species from the Antilles (*T. swalesi* from Hispaniola and *T. lherminieri* from Dominica), and is further subdivided into two main subclades corresponding to highland and lowland species, respectively.

The topology based on 49 additional loci (Fig. S4) includes a concatenated matrix of 65,574 bp, using a taxon set with 105 individuals. Boostrap (BS) support for a monophyletic *Turdus* is 100% (Fig. S4). *Turdus viscivorus* is sister to the remainder of the clade with strong support. The next lineage to diverge is *T. philomelos*, which in turn is sister to the remainder of the clade. A basal split separates two clades with low BS support values – one large group includes species from the Palaearctic, Africa, Nearctic, Panamanian, as well as the Antillean regions, and is sister to a group which includes species from the Antilles (*T. swalesi* and *T. lherminieri*) and all samples from the continental South America Region (Fig. S4, weakly supported). Support for a monophyletic African radiation is strong, and *T. swalesi* and *T. lherminieri* are recovered (although with weak support) as part of the Neotropical radiation, as for the UCE data set (Node E, Fig. 1, Fig. S2 and Fig. S3).

The analysis of the cyt*b* data set (Fig. S5) recovers a monophyletic *Turdus* clade (excluding *Otocichla mupinensis* and *Psophocichla litsitsirupa*, which were recovered as sisters to the *Turdus* clade and which have both previously been included in *Turdus*), where *T. viscivorus* and *T. philomelos* are again the first lineages to diverge, being sisters to the remainder of the clade with high support. Within the main clade, most early diverging nodes are unsupported, but otherwise there are many similarities to previous studies [2, 3]. African species are divided into six clades, with *T. pelios* sister to Antillean species and a Eurasian clade with the exception of *T. merula* and *T. iliacus.* Unlike previous studies [2, 3], there is for the first time high support for a monophyletic South American clade based on a single mitochondrial locus. A number of unexpectedly deep or shallow divergences of potential taxonomic interest are highlighted in Fig. S5 and discussed in the supplementary material.

The UCE species tree (Fig. S6, with gene trees of 483 UCE loci as input in ASTRAL) recovers a similar topology to the concatenated UCEs and cyt*b* regarding *T. viscivorus* and *T. philomelos*. The placement of these species was also recovered, although in reverse order compared to concatenated UCEs and cyt*b*. Here, *T. viscivorus* and *T. philomelus* are sisters to a strongly supported clade, which consists of two major groups: one including Panamanian, Western Palaearctic, Antillean, African, Eastern Palaearctic; and one South American group (Node D, Fig. 1), with a few Panamanian and Antillean species, plus two Eastern Palaearctic species, *Turdus eunomus* and *T. naumanni*. Support for the diverging order is weak, but several of the same groups as in Fig. 1 are recovered with strong support, e.g. *T. plebejus*, the Central American clade (*T. rufitorques, T. nigrescens, T. infuscatus, T. migratorius*), the African clade and the Eurasian clade. Also, the Neotropical clade is similar to the topology in Fig. 1, including the division between the highland and lowland clades.

The UCE species tree (Fig. S7, with 1,931 UCE loci as input in SVDquartets) shows *T. lherminieri* from the Antilles as sister species to all other species of the crown group. Again, this analysis recovers most of the same clades as the other analyses performed in this study, while there is no resolution regarding the phylogenetic relationships among these large groups. The similarities between analyses are the recovery of a monophyletic African group, a monophyletic Eurasian group, a monophyletic Panamanian group and a generally similar Neotropical clade.

The species tree built from the 49 additional loci (Fig. S8) (with gene trees of each additional locus as input) recovers a tree topology where the species *Turdus viscivorus* and *T. philomelos* are again the first to diverge, followed by two main groups (Fig. S8): a moderately supported Afrotropical clade sister to the remainder of the thrushes from all non-African regions. In this tree, the main topology is insufficiently supported, but major clades such as the Eurasian clade including *T. iliacus* and *T. merula* are recovered, although support is weak. The American radiation is recovered as monophyletic, but again with weak support. Although there are differences in detail, major patterns in the Panamanian and Neotropical clades proposed by previous analyses shown here are corroborated.

Divergence time estimates

The crown age of *Turdus* is estimated to c. 9.3 million years (Ma) (Fig. 3, Fig. S9), in late Miocene. The first event of the major global radiation starts c. 7.2 million years ago (Mya), corresponding to the divergence of the African clade, rapidly followed by the divergence at c. 5.7 Mya between the Palaearctic and Oriental clades from the clade comprising species with distributions in the New World. Around 5.3 Mya, the New World

radiation begins. Panamanian and South American clades first begin to diverge at c. 4.4 Mya and 4.9 Mya, respectively.

Geographical ancestral range reconstruction

Including the "jump dispersal" (j) parameter in the DEC model (Fig. 3), implemented in BioGeoBEARS, suggests a similar scenario as the DEC reconstruction (not shown), but causes the reconstructions at the nodes to become less noisy. Independent dispersals originating in the Western Palaearctic and moving towards the Eastern Palaearctic continuing to the Oriental region are suggested. The reconstruction of the New World radiation (including N, C, GA and SA, see Fig. 3 for abbreviations) suggests that it originated from a single dispersal event from the Western Palaearctic to the Antilles, although weak clade support makes this conclusion tentative (Fig. 1). From the Antilles, one or two dispersals to the Central America region are inferred, but the interpretation is complicated. From the Panamanian region, one lineage (*T. migratorius*) was recovered to have dispersed to North America. The radiation in South America is inferred to have originated directly from an ancestor dispersing from the Great Antilles. Separate dispersals back to the Central America region from South America are implied for the ancestors of *T. assimilis* and *T. grayi* (Fig. 3).

Discussion

Data considerations

The different evolutionary scenarios that have been suggested by studies of *Turdus* [2, 3] propose conflicting scenarios of how they spread across the world. Most likely, the main reasons for the discrepancies are the differences in the amount and source of genetic data, combined with the stochasticity introduced by the short internodes caused by the high rate of speciation during the radiation. The UCE topology (ML) with 1,931 concatenated loci (75% completeness of taxa) is the best currently available overview of the *Turdus* radiation, due to the highest number of loci sampled and the better resolution recovered to date (Fig. 1 and Fig. S2). The concatenated UCE dataset shows reduced incongruence and improved resolution of the topology, as already documented for this kind of approach [20]. The more limited genetic sampling used by Voelker *et al*. [2] and Nylander *et al*. [3] makes these analyses more vulnerable to disagreement between the genealogy of the loci analysed and the species tree, as well as to the effects of various evolutionary processes such as incomplete lineage sorting, gene flow and hybridization. By exploring the different kinds of datasets obtained by genomic sampling, we were able to estimate a novel phylogenetic hypothesis based on 1,931 UCEs (Fig. 1, Fig. S2 and Fig. S3). These data suggest a much simpler and parsimonious dispersal scenario compared to previous studies.

Divergence time estimates

The age of the split between *Oenanthe* and *Turdidae* was estimated to 22 Mya, corresponding to the upper extent of the confidence limit given for this split in Fig. 2 in Oliveros *et al*. [16]. This place the radiation of Turdidae within a time frame compatible with several recent studies [16, 21-24]. Furthermore, the age of divergences between species are also compatible with the standard 2,1% per million years divergence rate in the cytochrome b gene [25].

Phylogenetic implications and the historical biogeography of *Turdus*

Our time-calibrated phylogeny based on 1,931 UCEs (Fig. 3, Fig. S9) sheds new light on the relationships among the majority of species in the genus *Turdus*. Previous studies suggested a series of trans-Atlantic dispersal events, both from Africa to the New World and from the Caribbean Islands to the Old World. Our findings challenge these hypotheses and that the

African thrushes acted as a source for dispersal to the New World [3, 26], and suggest a different scenario for the evolution of the genus *Turdus*. Although we cannot completely rule out the possibility of more than one trans-Atlantic dispersal (see *Phylogenetic incongruences leading to alternative phylogenetic histories* in the electronic supplementary material), the topologies allowing for more than one transatlantic dispersal are unsupported in that respect, and in some details most likely spurious. Our statistically most well supported results based on 1,931 UCEs differ most importantly from previous hypotheses in that i) the African radiation is monophyletic; ii) Eurasian taxa did not originate from a west to east transatlantic dispersal; and iii) that the American taxa originate from a single dispersal from the Old World (Western Palaearctic) to the Americas, a result recovered also with low support in the analysis of 49 independent loci.

Ancestral lineages are here inferred to having occurred in the Western Palaearctic, and from there, dispersals to the Afrotropical, Eastern Palaearctic and South American regions took place. The Afrotropical radiation is inferred to have been entirely *in situ*, with no indication that it had any role in the colonization of South America (Fig. 3, Fig. S9). The radiation in the Old World seems to have originated in the Western Palaearctic, with a subsequent spread towards the Eastern Palaearctic and Oriental regions on at least two separate occasions (Fig. 3, Fig. S9). We note, however, that genomic sampling of Palaearctic species is incomplete, making these conclusions tentative. Contrary to previous hypotheses, *Turdus pelios* is recovered in the African clade and is no longer suggested to be more closely related to species from the Caribbean (Fig.2, Fig. 3), thus contradicting both a close relationship with other taxa from South America [2] as well as a reversed transatlantic dispersal event, as inferred by both Nylander *et al*. [3] and Voelker *et al*. [2]. *T. philomelos* and *T. viscivorus* represent ancient lineages that seem to have been unaffected by the processes driving the global radiation from the Palaearctic region (Fig. 1 and Fig. 3, Fig. S2-S9). *Turdus iliacus* is inferred to be sister to *T. merula* and both are part of the Palaearctic clade, with strong support. In contrast, both Voelker *et al*. [2] and Nylander *et al*. [3] recovered *T. iliacus* within the New World clade, as sister to *T. plebejus*, a Panamanian species.

We find evidence for the Antilles as the location of the first colonization event (Fig. 3). In the ancestral range reconstruction shown in Fig. 3, an Antillean distribution receives the highest probability, but Central America is also a possibility. *Turdus* thus seems to be an example of a long-distance dispersal from the Palaearctic where the birds first settled in the Caribbean region and then proceeded to radiate and colonize the mainland. These new data receive higher phylogenetic support than previous studies, and generate a both more parsimonious explanation and a more logical scenario for the colonization of the Americas by *Turdus.*

The initial events in the colonisation of the Americas seem to be centred around the Caribbean region. The most likely scenario according to the ancestral range reconstruction (Fig. 3) is a dispersal from a founder population in the Greater Antilles to Central America, resulting in one limited radiation including the ancestors of the *T. rufitorques* clade and in the *T. plebejus* lineage, followed by a reverse dispersal back to the Antilles from the Panamanian region by the ancestors of *T. swalesi* and *T. lherminieri*. In an alternative scenario, including two dispersals from the Greater Antilles to the Panamanian region, the ancestor of the clade including *T. rufitorques* would have had to disperse first, followed by the ancestor of *T. plebejus*, while the ancestors of *T. swalesi* and *T. lherminieri* would emanate from dispersal events within the Antilles.

Thrushes probably entered the Panamanian region by the time a land bridge was already fully or partly established [27-29]. There is an ongoing debate on the emergence of the Panamanian land bridge and the timing and processes underlying the Great American Biotic Interchange [29], which is partly due to difficulties in the interpretation of the exposure of land and shallow waters [28]. The closure of the Panamanian land bridge has had an important impact on the diversification of a variety of New World birds, as shown by Smith and Klicka [30]. Weir *et al*. [31], Töpel *et al*. [32], Antonelli *et al*. [33], Oliveros *et al*. [34], among others, have shown a marked increase in the rates of interchange of South and Central American birds, after or in connection with a land bridge completion. These studies suggest that the route of most dispersal events was primarily south to north.

Whilst a common pattern for birds, thrushes are likely to only have been marginally affected by the emergence of the Panamanian uplift. The colonization of South America is instead inferred to be a dispersal event directly from the Antilles, with no evidence of any connection to the Panamanian land bridge. This is not surprising, since these birds evidently dispersed to and between the Antillean islands, and could thus have dispersed between the Panamanian or Antillean regions and continental South America independently of a land bridge. This result shows similarities to findings from studies of other taxa. For instance, Sturge *et al*. [35] showed, based on mitochondrial DNA (cytochrome b and ND2), that the colonization of South America by New World orioles (*Icterus*) is likely to have involved ancestors from the Caribbean, and a recent biogeographical reconstruction recovered reverse colonization by short-faced bats from the islands (e.g. Antilles) to South America [36]. Other examples include the genus *Megascops* (Aves, Strigidae) endemic to the New World with a likely origin in the Caribbean Islands [37].

By improving the taxonomic and geographic sampling within South America, we recovered for the first time a single, monophyletic South American clade within *Turdus*. In contrast, Nylander *et al*. [3] inferred three South American clades, and thus suggested independent colonization events. Our results regarding the South American radiation are similar to those of Voelker *et al*. [2] in this respect, apart from the African species (*T. pelios*) that was part of the American clade in their analysis but is part of the African clade in this study (Fig. 1, Fig. 2, Fig. S2).

According to our phylogenetic hypothesis, the South American clade is divided into two main groups. One comprises mainly highland species (mostly Andean and Tepuian, but one Atlantic Forest species) and corresponds to an Andean clade already identified in Voelker, Rohwer [2]. The second main clade includes species from the lowlands in Amazonia, Chaco, Cerrado and Pampas, as well as Central America (*T. grayi* and *T. assimilis*). Paraphyly of *T. olivater* was detected, with *T. olivater kemptoni* (U4322, Venezuela) being recovered as sister to *T. fuscater fuscater* (U4285, Bolivia) and the Tepuian *T. olivater roraimae* sister to these two. This pattern has been documented in a previous study using a multilocus dataset [37]. Similarly, *T. fuscater* appears as paraphyletic, with *T. fuscater gigantoides* (U4287, Peru) being sister to *T. chiguanco conradi* (U4279, Peru) [38]. From continental South America, a number of independent reversals – dispersal events to both the Antilles and the Panamanian region – are inferred, which in the latter case could have been aided by the land bridge.

Future studies could focus on clarifying the geographical range evolution of *Turdus* within South America and along altitudinal zones, as well as investigating the influence of landscape and climatic changes on their past and current distribution and genetic diversity.

Conclusions

By employing broad genomic data with dense taxonomic sampling (see Fig. S10 for an overview of all approaches used in this study), we were able to not only provide an improved phylogenomic framework for continued taxonomy and classification revisions, but also a starting point for more detailed studies of the morphological, behavioural and ecological evolution in thrushes. In addition, our results provide strong evidence to reconsider ongoing controversies on the early evolution and range evolution of *Turdus*, including the logical but novel inference of a monophyletic *in situ* radiation in Africa, no American origin of the major Palaearctic radiation and a single rather than multiple trans-Atlantic dispersals giving rise to the American radiation. In summary, phylogenomic analyses are not only useful at higher taxonomic levels [39], but also hold the potential to uncover new insights into the diversification and biogeographic history of rapid species radiations.

References

[1] del Hoyo, J., Elliott, A., Sargatal, J., Christie, D.A. & Kirwan, G. 2019 *Handbook of the Birds of the World Alive*, Lynx Edicions.

[2] Voelker, G., Rohwer, S., Bowie, R.C.K. & Outlaw, D.C. 2007 Molecular systematics of a speciose, cosmopolitan songbird genus: Defining the limits of, and relationships among, the Turdus thrushes. *Molecular Phylogenetics and Evolution* **42**, 422-434. (doi:10.1016/j.ympev.2006.07.016).

[3] Nylander, J.A., Olsson, U., Alstrom, P. & Sanmartin, I. 2008 Accounting for phylogenetic uncertainty in biogeography: a Bayesian approach to dispersal-vicariance analysis of the thrushes (Aves: Turdus). *Syst Biol* **57**, 257-268. (doi:10.1080/10635150802044003).

[4] Nagy, J., Végvári, Z. & Varga, Z. 2019 Phylogeny, migration and life history: filling the gaps in the origin and biogeography of the Turdus thrushes. *Journal of Ornithology* **160**, 529-543. (doi:10.1007/s10336-019-01632-3).

[5] Melo, M., Bowie, R.C.K., Voelker, G., Dallimer, M., Collar, N.J. & Jones, P.J. 2010 Multiple lines of evidence support the recognition of a very rare bird species: the Príncipe thrush. *Journal of Zoology*, no-no. (doi:10.1111/j.1469-7998.2010.00720.x).

[6] Núñez-Zapata, J. & Peterson, A.T. 2016 Pleistocene diversification and speciation of White-throated Thrush (Turdus assimilis; Aves: Turdidae). *Journal of Ornithology*.

[7] Cerqueira, P.V., Santos, M.P.D. & Aleixo, A. 2016 Phylogeography, inter-specific limits and diversification of Turdus ignobilis (Aves: Turdidae). *Mol Phylogenet Evol* **97**, 177-186. (doi:10.1016/j.ympev.2016.01.005).

[8] Avendano, J.E., Arbelaez-Cortes, E. & Cadena, C.D. 2017 On the importance of geographic and taxonomic sampling in phylogeography: A reevaluation of diversification and species limits in a Neotropical thrush (Aves, Turdidae). *Mol Phylogenet Evol* **111**, 87-97. (doi:10.1016/j.ympev.2017.03.020).

[9] Bowie, R.C.K., Bloomer, P., Clancey, P.A. & Crowe, T.M. 2003 The Karoo Thrush (Turdus smithi Bonaparte 1850), a southern African endemic. *Ostrich* **74**, 1-7. (doi:10.2989/00306520309485364).

[10] Faircloth, B.C., McCormack, J.E., Crawford, N.G., Harvey, M.G., Brumfield, R.T. & Glenn, T.C. 2012 Ultraconserved elements anchor thousands of genetic markers spanning multiple evolutionary timescales. *Syst Biol* **61**, 717-726. (doi:10.1093/sysbio/sys004).

[11] Backström, N., Fagerberg, S. & Ellegren, H. 2008 Genomics of natural bird populations: a gene-based set of reference markers evenly spread across the avian genome. *Mol Ecol* **17**, 964-980. (doi:10.1111/j.1365-294X.2007.03551.x).

[12] Stamatakis, A. 2014 RAxML version 8: a tool for phylogenetic analysis and post-analysis of large phylogenies. *Bioinformatics* **30**, 1312-1313. (doi:10.1093/bioinformatics/btu033).

[13] Seo, T.K. 2008 Calculating bootstrap probabilities of phylogeny using multilocus sequence data. *Mol Biol Evol* **25**, 960-971. (doi:10.1093/molbev/msn043).
[14] Mirarab, S., Reaz, R., Bayzid, M.S., Zimmermann, T., Swenson, M.S. & Warnow, T. 2014 ASTRAL: genome-scale coalescent-based species tree estimation. *Bioinformatics* **30**, i541-548. (doi:10.1093/bioinformatics/btu462).
[15] Chifman, J. & Kubatko, L. 2014 Quartet inference from SNP data under the coalescent model. *Bioinformatics* **30**, 3317-3324. (doi:10.1093/bioinformatics/btu530).
[16] Oliveros, C.H., Field, D.J., Ksepka, D.T., Barker, F.K., Aleixo, A., Andersen, M.J., Alström, P., Benz, B.W., Braun, E.L., Braun, M.J., et al. 2019 Earth history and the passerine superradiation. *Proceedings of the National Academy of Sciences*, 201813206. (doi:10.1073/pnas.1813206116).
[17] Smith, S.A. & O'Meara, B.C. 2012 treePL: divergence time estimation using penalized likelihood for large phylogenies. *Bioinformatics* **28**, 2689-2690. (doi:10.1093/bioinformatics/bts492).
[18] Matzke, N.J. 2014 Model selection in historical biogeography reveals that founder-event speciation is a crucial process in Island Clades. *Syst Biol* **63**, 951-970. (doi:10.1093/sysbio/syu056).
[19] Holt, B.G., Lessard, J.-P., Borregaard, M.K., Fritz, S.A., Araújo, M.B., Dimitrov, D., Fabre, P.-H., Graham, C.H., Graves, G.R., Jønsson, K.A., et al. 2013 An Update of Wallace's Zoogeographic Regions of the World. *Science* **339**, 74-78. (doi:10.1126/science.1228282).
[20] Salichos, L. & Rokas, A. 2013 Inferring ancient divergences requires genes with strong phylogenetic signals. *Nature* **497**, 327-331. (doi:10.1038/nature12130).
[21] Claramunt, S. & Cracraft, J. 2015 A new time tree reveals Earth history's imprint on the evolution of modern birds. *Sci Adv* **1**, e1501005. (doi:10.1126/sciadv.1501005).
[22] Moyle, R.G., Oliveros, C.H., Andersen, M.J., Hosner, P.A., Benz, B.W., Manthey, J.D., Travers, S.L., Brown, R.M. & Faircloth, B.C. 2016 Tectonic collision and uplift of Wallacea triggered the global songbird radiation. *Nat Commun* **7**, 12709. (doi:10.1038/ncomms12709).
[23] Prum, R.O., Berv, J.S., Dornburg, A., Field, D.J., Townsend, J.P., Lemmon, E.M. & Lemmon, A.R. 2015 A comprehensive phylogeny of birds (Aves) using targeted next-generation DNA sequencing. *Nature* **526**, 569-573. (doi:10.1038/nature15697).
[24] Selvatti, A.P., Gonzaga, L.P. & Russo, C.A. 2015 A Paleogene origin for crown passerines and the diversification of the Oscines in the New World. *Mol Phylogenet Evol* **88**, 1-15. (doi:10.1016/j.ympev.2015.03.018).
[25] Weir, J.T. & Schluter, D. 2008 Calibrating the avian molecular clock. *Mol Ecol* **17**, 2321-2328. (doi:10.1111/j.1365-294X.2008.03742.x).
[26] Voelker, G., Rohwer, S., Outlaw, D.C. & Bowie, R.C.K. 2009 Repeated trans-Atlantic dispersal catalysed a global songbird radiation. *Global Ecology and Biogeography* **18**, 41-49. (doi:10.1111/j.1466-8238.2008.00423.x).
[27] Montes, C., Cardona, A., McFadden, R., Moron, S.E., Silva, C.A., Restrepo-Moreno, S., Ramirez, D.A., Hoyos, N., Wilson, J., Farris, D., et al. 2012 Evidence for middle Eocene and younger land emergence in central Panama: Implications for Isthmus closure. *Geological Society of America Bulletin* **124**, 780-799. (doi:10.1130/b30528.1).
[28] Bacon, C.D., Silvestro, D., Jaramillo, C., Smith, B.T., Chakrabarty, P. & Antonelli, A. 2015 Biological evidence supports an early and complex emergence of the Isthmus of Panama. *Proceedings of the National Academy of Sciences* **112**, 6110-6115. (doi:10.1073/pnas.1423853112).
[29] Jaramillo, C., Montes, C., Cardona, A., Silvestro, D., Antonelli, A. & Bacon, C.D. 2017 Comment (1) on "Formation of the Isthmus of Panama" by O'Dea et al. *Sci Adv* **3**, e1602321. (doi:10.1126/sciadv.1602321).

[30] Smith, B.T. & Klicka, J. 2010 The profound influence of the Late Pliocene Panamanian uplift on the exchange, diversification, and distribution of New World birds. *Ecography*. (doi:10.1111/j.1600-0587.2009.06335.x).
[31] Weir, J.T., Bermingham, E. & Schluter, D. 2009 The Great American Biotic Interchange in birds. *Proceedings of the National Academy of Sciences* **106**, 21737-21742. (doi:10.1073/pnas.0903811106).
[32] Töpel, M., Zizka, A., Calio, M.F., Scharn, R., Silvestro, D. & Antonelli, A. 2017 SpeciesGeoCoder: Fast Categorization of Species Occurrences for Analyses of Biodiversity, Biogeography, Ecology, and Evolution. *Syst Biol* **66**, 145-151. (doi:10.1093/sysbio/syw064).
[33] Antonelli, A., Zizka, A., Carvalho, F.A., Scharn, R., Bacon, C.D., Silvestro, D. & Condamine, F.L. 2018 Amazonia is the primary source of Neotropical biodiversity. *Proc Natl Acad Sci U S A*. (doi:10.1073/pnas.1713819115).
[34] Oliveros, C.H., Andersen, M.J., Hosner, P.A., Mauck, W.M., Sheldon, F.H., Cracraft, J. & Moyle, R.G. 2019 Rapid Laurasian diversification of a pantropical bird family during the Oligocene-Miocene transition. *Ibis*. (doi:10.1111/ibi.12707).
[35] Sturge, R.J., Jacobsen, F., Rosensteel, B.B., Neale, R.J. & Omland, K.E. 2009 Colonization of South America from Caribbean Islands Confirmed by Molecular Phylogeny with Increased Taxon Sampling. *The Condor* **111**, 575-579. (doi:10.1525/cond.2009.080048).
[36] Tavares, V.d.C., Warsi, O.M., Balseiro, F., Mancina, C.A. & Dávalos, L.M. 2018 Out of the Antilles: Fossil phylogenies support reverse colonization of bats to South America. *Journal of Biogeography* **45**, 859-873. (doi:10.1111/jbi.13175).
[37] Dantas, S.M., Weckstein, J.D., Bates, J.M., Krabbe, N.K., Cadena, C.D., Robbins, M.B., Valderrama, E. & Aleixo, A. 2016 Molecular systematics of the new world screech-owls (Megascops: Aves, Strigidae): biogeographic and taxonomic implications. *Mol Phylogenet Evol* **94**, 626-634. (doi:10.1016/j.ympev.2015.09.025).
[38] Valderrama, E., Pérez-Emán, J.L., Brumfield, R.T., Cuervo, A.M., Cadena, C.D. & Patten, M. 2014 The influence of the complex topography and dynamic history of the montane Neotropics on the evolutionary differentiation of a cloud forest bird (Premnoplex brunnescens, Furnariidae). *Journal of Biogeography* **41**, 1533-1546. (doi:10.1111/jbi.12317).
[39] Zhang, G. & Li, C. & Li, Q. & Li, B. & Larkin, D.M. & Lee, C. & Storz, J.F. & Antunes, A. & Greenwold, M.J. & Meredith, R.W., et al. 2014 Comparative genomics reveals insights into avian genome evolution and adaptation. *Science* **346**, 1311-1320. (doi:10.1126/science.1251385).

Data accessibility

All DNA sequence data produced in this project are made freely available at NCBI Sequence Read Archive (SRA) under the BioProject accession PRJNA574741 (Table S1). The project's documentation, comprising origin of all data, download information, and basic information, is freely available on GitHub: https://github.com/RominaSSBatista/Turdus-Project.

Authors' contributions

R.B., C.R., A. Aleixo, A. Antonelli and U.O. conceived, designed and coordinated the study and helped draft the manuscript.; R.B and U.O carried out the molecular lab work; R.B., T.A and U.O participated in data analysis; R.B. led the writing with contributions from all authors. All authors gave final approval for publication.

Competing interests

The authors have no competing interests to declare.

Funding

This research was supported by the Knut and Alice Wallenberg Foundation through a Wallenberg Academy Fellowship, the Swedish Research Council, and the Swedish Foundation for Strategic research (grants to A.Antonelli); the US National Science Foundation [NSF DEB 1241056], Fundação de Amparo à Pesquisa do Estado de São Paulo [FAPESP 2012/50260-6] and CNPq [fellowships 306843/2016-1 to A.Aleixo and 308927/2016-8 to CCR]. Romina Batista received a Doctoral Fellowship and a Fellowship for Internship abroad from Coordination for the Improvement of Higher Education Personnel [CAPES, Processo 99999.000566/2015-02]. Genomic work was further supported by Science for Life Laboratory and the National Genomics Infrastructure funded by the Swedish Research Council.

Acknowledgments

We thank the curator and curatorial assistants of Burke Museum (UWBM); American Museum of Natural History (AMNH); Louisiana State University Museum of Natural Science (LSUMZ); South Western Forestry University (SWFU); Zoological Museum, University of Copenhagen (ZMUC); Naturhistoriska riksmuseet (NRM); Department of Biology and Environmental Science, University of Gothenburg (DZUG); Göteborg Naturhistoriska Museum (GNM and GNM-Av.ex); Martim Melo collection; Instituto Nacional de Pesquisas da Amazônia (INPA); Laboratório de Genética e Evolução Molecular de Aves (LGEMA); Divisão de Aves do Museu de Zoologia da Universidade Estadual de Feira de Santana (DAMZUFS) and Museu Paraense Emílio Goeldi (MPEG), for loaning tissue samples (Table S1). We thank the Uppsala Multidisciplinary Center for Advanced Computational Science for assistance with massively parallel sequencing and access to the UPPMAX computational infrastructure. Bioinformatics analyses were run on the Albiorix computer cluster (http://albiorix.bioenv.gu.se/) at the University of Gothenburg. The authors also acknowledge the National Laboratory for Scientific Computing (LNCC/MCTI, Brazil) for providing HPC resources of the SDumont supercomputer, which have contributed to the research results reported within this paper. We also thank Anna Ansebo for her support in the entire process of the wet lab; Mats Töpel, for his support with bioinformatics and constructive advice that greatly improved the data process. The first author also thanks Chrysoula Gubili, Erico Polo, and Mateus Ferreira for helpful comments and guidance toward improving the manuscript.

Figure legends

Figure 1. Phylogenies of *Turdus.* Topology with branch lengths, based on concatenated maximum likelihood analysis of 1,931 UCE loci. Numbers on nodes indicate maximum likelihood bootstrap support. Nodes without numbers indicate maximum likelihood bootstrap support > 75%. Letters A-E depict the main nodes mentioned in the text. Branch in red represent a historical sample (toepads) included in this study. Zoogeographical regions, according to the current distribution of *Turdus* species, are provided to the right of the tree. Shaded boxes in grey show the subdivision of Old/New World areas and two main groups within South America (highland and lowland).

Figure 2. Biogeographic hypotheses for *Turdus*. Summarized from (a) Voelker *et al*., 2007 (2 mitochondrial genes), asterisks above nodes indicate Bayesian posterior probability ≥ 0.95, numbers below nodes indicate maximum likelihood bootstrap support (>50%); (b) Nylander *et al*., 2008 (2 mitochondrial and 2 nuclear genes), numbers above nodes indicate posterior

probability (>0.95); (c) This study (genomic sampling of 1,931 UCEs), numbers below nodes indicate maximum likelihood bootstrap values. Only major clades are shown.

Figure 3. Ancestral range reconstruction. *Turdus* time-calibrated phylogeny, based on 1,931 UCEs, calibrated with one fossil calibration (black arrow), and with range evolution estimated under the DEC+j model. Pie charts show the probability of each range. All nodes including secondary colours represent the uncertainty to recover a unique ancestral range for certain nodes within the phylogeny. The map shows the biogeographical regions used for the analyses (adapted from Holt et al., 2013).

Table S1. List of taxa, locality and voucher information.

ID	Species	Museum	Voucher	Tissue Number	Country	Locality	lat	lonw	Level	Tyne	NCBI
U4172	*Turdus infuscatus* Lafresnaye, 1844	Burke Museum	UWBM 104375	DAB 4706	Guatemala	Departamento de Totonicapan, mountains nearest Totonicapan	14.9108	-91.36056	INGROUP	Tissue	SAMN12984381
U4189	*Turdus plebejus plebejus* Cabanis, 1861	Burke Museum	UWBM 113247	JK 07 503	Panama	Provincia de Chiriqui, Parque Nacional Volcan Baru	8.8449	-82.53938	INGROUP	Tissue	SAMN12984382
U4159	*Turdus albicollis assimilis* Cabanis, 1850	Burke Museum	UWBM 104255	DHB 4586	Guatemala	Departamento de Quetzaltenango Santa Maria de Jesus 5 km SSW Finca de Santa Maria	14.8319	-91.51669	INGROUP	Tissue	SAMN12984383
U4162	*Turdus anthracinus* Burmeister, 1858	Burke Museum	UWBM 54433	DAB 837	Argentina	Provincia de Tucuman, San Miguel de Tucuman, El Infiernillo	-26.75	-65.74	INGROUP	Tissue	SAMN12984384
U4164	*Turdus ravidi ravidi* Bonaparte, 1838	Burke Museum	UWBM 104010	DHB 4341	Guatemala	Departamento de Retalhuleu, San Feline Retalhuleu, 5 km S. Finca El Nino	14.6206	-91.59611	INGROUP	Tissue	SAMN12984385
U4168	*Turdus grayi lamyoni* A. R. Phillips, 1966	Burke Museum	UWBM 100667	BTS 07 160	Mexico	Campeche, Municipio de de la Candelaria	19.3304	-99.14631	INGROUP	Tissue	SAMN12984386
U4177	*Turdus libonyana libonyana* A. Smith, 1836	Burke Museum	UWBM 52923	SAR 6744	South Africa	KwaZulu/Natal Province, Melmoth	-28.59	31.44	INGROUP	Tissue	SAMN12984387
U4273	*Turdus amaurochalinus* Cabanis, 1850	Louisiana State University Museum of Natural Science	LSUMZ 37732		Bolivia	Santa Cruz Department. Dn Mario de Chiquiitos 126 km ENE San Jose	-17.7895	-63.18298	INGROUP	Tissue	SAMN12984388
U4334	*Turdus rubripes schistaceus* S. F. Baird, 1864	Louisiana State University Museum of Natural Science	LSUMZ 82992		Cuba	Guant namo Province, U.S. Guantanamo Naval Base Graffiti Hill	20,14	-75.2129	INGROUP	Tissue	SAMN12984389
U4342	*Turdus ruficrentris rufiventris* Vieillot, 1818	Louisiana State University Museum of Natural Science	LSUMZ 31619		Bolivia	Santa Cruz Department. Prov. El Tambo 14 km SE Comarana 18 dearees 00' 23" S 64 dearees 2(	-18.0064	-64.435	INGROUP	Tissue	SAMN12984390
U2338	*Turdus torquatus amaurolaimus* Hartert, 1923	Department of Biology and Environmental Science, University of Gothenburg	DZUG 1338		Armenia	Aranats 2007-06-04, PJL	40.5232	44.19463	INGROUP	Tissue	SAMN12984391
U4176	*Turdus libonyana libonyana* A. Smith, 1836	Burke Museum	UWBM 67035	LKB 118	South Africa	KwaZulu/Natal Province, Melmoth, Saxony Farm	-28,61	31,375	INGROUP	Tissue	SAMN12984392
U4345	*Turdus serranus fuscobrunneus* (Chapman, 1912)	Louisiana State University Museum of Natural Science	LSUMZ 12152		Ecuador	Pichincha Province. MINDO	-0.04896	-78.77524	INGROUP	Tissue	SAMN12984393
U4325	*Turdus obscurus* J. F. Gmelin, 1789	Louisiana State University Museum of Natural Science	LSUMZ 16993		Japan	Wakayama Prefecture, Gobo	33.8915	135.15235	INGROUP	Tissue	SAMN12984394
U3899	*Turdus rufitorques* Hartlaub. 1844	Louisiana State University Museum of Natural Science	LSUMZ B-60971		Honduras	Francisco Morazán Department. Cerro UYUCA.zamorano Bio logical research station	14.0167	-87.08333	INGROUP	Tissue	SAMN12984395
U4320	*Turdus obsoletus obsoletus* Lawrence. 1862	Louisiana State University Museum of Natural Science	LSUMZ 41621		Panama	Bocas del Toro Province. Chiriuni to Chiriuni Grande road	8.79139	-82.20984	INGROUP	Tissue	SAMN12984396
U4163	*Turdus amaurochalinus* Burmeister, 1858	Burke Museum	UWBM 92132	GAV 988	Argentina	Provincia de Jujuy, Tilcara	-24.1843	-65.30218	INGROUP	Tissue	SAMN12984397
U4319	*Turdus obsoletus narambanus* Hartert. 1920	Louisiana State University Museum of Natural Science	LSUMZ 11711		Ecuador	Esmeraldas Province. EL PLACER CA 670M	-2.81047	-79.98909	INGROUP	Tissue	SAMN12984398
U4331	*Turdus pilaris* Linnaeus, 1758	Louisiana State University Museum of Natural Science	LSUMZ 1330		Denmark	Vestjaelland County, Soro Amt 3 km SE Korsor	55.3258	11.149389	INGROUP	Tissue	SAMN12984399
U4330	*Turdus nhilomelos clarkei* Hartert. 1909	Louisiana State University Museum of Natural Science	LSUMZ 12244		Sweden	Provance Oland Ottenby Bird Station	56.1977	16.399458	INGROUP	Tissue	SAMN12984400
U4337	*Turdus noliocephalus vanikorensis* Ouov & Gaimard. 1830	Louisiana State University Museum of Natural Science	LSUMZ 45823		Vanuatu	Esniritu Santo 1.5 km SE Wusi	-15.3783	167.66167	INGROUP	Tissue	SAMN12984401
U4322	*Turdus olivater kemptoni* Phelps, Sr & Phelps, Jr, 1955	Louisiana State University Museum of Natural Science	LSUMZ 7399		Venezuela	Amazonas Territory, CERRO DE LA NEBLINA CAMP VII 1800M	0.32396	-65.7748	INGROUP	Tissue	SAMN12984402
U4155	*Turdus amaurochalinus* Cabanis, 1850	Burke Museum	UWBM 54448	DAB 859	Argentina	Provincia de Corrientes, Corrientes. Manuel Derqui	-27.8419	-58.81194ae	INGROUP	Tissue	SAMN12984403
U4336	*Turdus poliocephalus xanthonhrys* (Sharpe, 1888)	Louisiana State University Museum of Natural Science	LSUMZ 52693		Malaysia	Sabah, Tambunan district Mt. Kinabalu Laban Rata	6.06444	116.57694	INGROUP	Tissue	SAMN12984404
U4339	*Turdus reevei* Lawrence. 1869	Louisiana State University Museum of Natural Science	LSUMZ 61301		Peru	Piura Department. Ouebrada Caballito 3 km NE El Tocto	-5.78593	-79.67617	INGROUP	Tissue	SAMN12984405
U4279	*Turdus chiguanco conradi* Salvadori & Festa. 1899	Louisiana State University Museum of Natural Science	LSUMZ 63070		Peru	Puno Department. 14Km NW Camno 15 Dearees 16.55'S 70Dearees 28.27'W	-15.275	-70.47117	INGROUP	Tissue	SAMN12984406
U4305	*Turdus migratorius achrusterus* (Batchelder, 1900)	Louisiana State University Museum of Natural Science	LSUMZ 70072		United States of America	Florida, Gainesville UF Campus	29.6415	-82.33856	INGROUP	Tissue	SAMN12984407
U4292	*Turdus hauhochrous* Todd. 1931	Louisiana State University Museum of Natural Science	LSUMZ 7620		Bolivia	Beni Department. 38K W TRINIDAD 175M	-14.8258	-64.90003	INGROUP	Tissue	SAMN12984408
U4297	*Turdus leucomelas leucomelas* Vieillot, 1818	Louisiana State University Museum of Natural Science	LSUMZ 14719		Bolivia	Santa Cruz Department, Serrania de Huanchaca 21km SE Cataratа Arco Iris	-14,5	-60,65	INGROUP	Tissue	SAMN12984409
U4285	*Turdus fuscater fuscater* Lafresnaye and d'Orbiany. 1837	Louisiana State University Museum of Natural Science	LSUMZ 22874		Bolivia	La Paz Department. Prov. B. Saavedra 83 km bv road E. Charazani Cerro Asunta Pata.	-14.7407	-68.39651	INGROUP	Tissue	SAMN12984410
U4329	*Turdus nhilomelos nhilomelos* C. L. Brehm. 1831	Louisiana State University Museum of Natural Science	LSUMZ 31164		Russia	Belarus: Dzerzhinsk Raion Fanival Sta	53.45	27.2	INGROUP	Tissue	SAMN12984411
U4281	*Turdus falcklandii magellanicus* P. P. King, 1831	Louisiana State University Museum of Natural Science	LSUMZ 14008		Chile	Magallanes y Antartica Chilena, Brunswick Peninsula near mouth of Rio Santa Maria ca 2 km S	-53.4833	-71.41687	INGROUP	Tissue	SAMN12984412
U4287	*Turdus fuscater sinuatodes* Cabanis. 1873	Louisiana State University Museum of Natural Science	LSUMZ 7673		Peru	Hulinuco Denartment. UNCHOG PASS NNW ACOMAYO 3450M	-13.924	-71.69326	INGROUP	Tissue	SAMN12984413
U4315	*Turdus nudigenis nudigenis* Lafresnaye, 1848	Louisiana State University Museum of Natural Science	LSUMZ 48523		Guyana	Region 9 Ireng River km Karasabai	3.88333	-59.58333	INGROUP	Tissue	SAMN12984414
U4179	*Turdus nigricans nigricens* (Seebohm, 1887)	Burke Museum	UWBM 92399	JAG 1919	Argentina	Provincia de Tucuman. Tafi del Valle. 20 km S. 6 km E	-26.8517	-65.70892	INGROUP	Tissue	SAMN12984415
U4314	*Turdus nigricans nigricens* Cabanis, 1874	Louisiana State University Museum of Natural Science	LSUMZ 43749		Peru	San Martin Department. Ca 22 km ENE Florida	-5.72306	-77.75026	INGROUP	Tissue	SAMN12984416
U4312	*Turdus nigricans nigricens* Cabanis, 1874	Louisiana State University Museum of Natural Science	LSUMZ 31511		Bolivia	Santa Cruz Department, Prov. Florida 23.2 km E Samaipata	-18,2775	-63.67444	INGROUP	Tissue	SAMN12984417
U4185	*Turdus olivaceus smithi* Bonanarte. 1850	Burke Museum	UWBM 95644	GAV 1777	South Africa	Northern Cape Province. Kimberlev. 95 km S. 45 km W	-29.6333	24.3	INGROUP	Tissue	SAMN12984418
U4338	*Turdus reevei* Lawrence, 1869	Louisiana State University Museum of Natural Science	LSUMZ 5151		Peru	Lambayeque Department, Las Pampas km 855 Pan-American Hwy 11 road km from Olmos	-6.38163	-79.52444	INGROUP	Tissue	SAMN12984419
U4317	*Turdus maculirostris* Berlepsch and Taczanowski, 1884	Louisiana State University Museum of Natural Science	LSUMZ 66432		Peru	Tumbes Department, Campo verde trail 3Degrees	-3.84567	-80.17642	INGROUP	Tissue	SAMN12984420
U4299	*Turdus maranonicus* Taczanowski. 1880	Louisiana State University Museum of Natural Science	LSUMZ 44756		Peru	Caiamarca Department. Las Juntas iunction nia Tabaconas and Chinchine	-5.38333	-78.77167	INGROUP	Tissue	SAMN12984421
U4309	*Turdus nigrescens* Cabanis, 1861	Louisiana State University Museum of Natural Science	LSUMZ 27265		Costa Rica	Cartago Province, 1 km N Villa Mills Cerro Abarca	9.86381	-83.91619	INGROUP	Tissue	SAMN12984422
U4321	*Turdus olivater roraimae* Salvin & Godman. 1884	Louisiana State University Museum of Natural Science	LSUMZ 48449		Guyana	S ulore Koniname Mountain 6 km W Kooinane	4.93333	-59.8	INGROUP	Tissue	SAMN12984423
U4192	*Turdus ruficrentris rufiventris* Vieillot, 1818	Burke Museum	UWBM 70177	DAB 858	Argentina	Provincia de Corrientes, Corrientes, Manuel Derqui	-27.8419	-58.8119	INGROUP	Tissue	SAMN12984424
U4170	*Turdus grayi megas* W. deW. Miller & Griscom, 1925	Burke Museum	UWBM 69222	DAB 1466	Nicaragua	Departamento de Managua, Managua, Chocovero	11.99	-86.26	INGROUP	Tissue	SAMN12984425
U4188	*Turdus plebejus plebejus* Cabanis. 1861	Burke Museum	UWBM 101022	BTS 08 009	Panama	Provincia de Chiriuni. Parque Nacional Volcan Baru	8.8449	-82.53938	INGROUP	Tissue	SAMN12984426
U4187	*Turdus plebejus rufaelenes* W. deW. Miller & Griscom, 1925	Burke Museum	UWBM 56119	DAB 1292	Nicaragua	Matagalpa	13.015	-85.924	INGROUP	Tissue	SAMN12984427
U4166	*Turdus ravidi cassius* (Bonanarte. 1855)	Burke Museum	UWBM 94374	DHB 2877	Honduras	Denartamento de Copan, Conan Ruinas. 10 km ENE	14.8333	-89.15	INGROUP	Tissue	SAMN12984428
U4194	*Turdus serranus serranus* Tschudi, 1844	Burke Museum	UWBM 73077	CVC 14	Bolivia	Departamento de Santa Cruz, Provincia Vallegrande, Vallegrande, San Lorenzo	-18,673	-63.9175	INGROUP	Tissue	SAMN12984429
U4352	*Turdus xanthorhynchus* Salvadori, 1901	Martim Melo collection	Not available		Gulf of Guinea	Principe	1.60498	7.3991472	INGROUP	Tissue	SAMN12984430
U4175	*Turdus libonyana troiscalis* W. K. H. Peters. 1881	Burke Museum	UWBM 104460	DHB 4791	Malawi	Southern Reaion. Mwanza. 20 km SW. Thanhami Forest Reserve	-15.4508	34.641403	INGROUP	Tissue	SAMN12984431
U4335	*Turdus plumbeus ardesiacus* Vieillot, 1822	Louisiana State University Museum of Natural Science	LSUMZ 11333		Puerto Rico	Cabo Roio Llanos Costa 0.5 km NNW mouth Arrovo Cazul	17.9899	-67.12987	INGROUP	Tissue	SAMN12984432
U4275	*Turdus albicollis assimilis* Cabanis. 1850	Louisiana State University Museum of Natural Science	LSUMZ 51425		Panama	Panamá Province. Cerro Campana Altos de Camnana Parque National W Canira	8.71372	-79.95284	INGROUP	Tissue	SAMN12984433
U4156	*Turdus amaurochalinus* Cabanis, 1850	Burke Museum	UWBM 70748	JAG 1820	Argentina	Provincia de Corrientes, Corrientes, Manuel Derqui	-27.8419	-58.8119ae	INGROUP	Tissue	SAMN12984434
U4190	*Turdus rufitorques* Hartlaub, 1844	Burke Museum	UWBM 104079	DHB 4410	Guatemala	Departamento de Quetzaltenango, Quezaltenango, Xela, El Baul	14,8283	-91,495	INGROUP	Tissue	SAMN12984435
U4282	*Turdus falvirostris* P. L. Sclater. 1858	Louisiana State University Museum of Natural Science	LSUMZ 33193		Peru	Caiamarca Department. Ca 3km NNE San Jose de Lourdes 5 dearees 04.3' S 78 dearees 57.9' W	-5.07167	-78.965	INGROUP	Tissue	SAMN12984436
TAM6	*Turdus amaurochalinus* Cabanis, 1850	Museu Paraense Emilio Goeldi	MPEG 70980 (T13720)	BR 364 012	Brazil	Rondonia, Jaciparaná	-9,36064	-64,65811	INGROUP	Tissue	SAMN12984437
TAM2	*Turdus amaurochalinus* Cabanis, 1850	Laboratório de Genética e Evolução Molecular de Aves	LGEMA 628	P230	Brazil	Pará. Parune Zoobotânico de Caraúis	-6.06139	-50.06	INGROUP	Tissue	SAMN12984438
TAL24	*Turdus albicollis* Vieillot, 1818	Museu Paraense Emilio Goeldi	MPEG 77372 (T20559)	SGC 310	Brazil	Amazonas, São Gabriel da Cachoeira PPBIO	-0,15	-66,8	INGROUP	Tissue	SAMN12984439
U1098	*Turdus pelios* Bonaparte, 1850	Louisiana State University Museum of Natural Science	LSUMZ 27170		Cameroon	Ouest Province, Airport at Tayandi, 20 km W Foumban	5,68038	10,877358	INGROUP	Tissue	SAMN12984440
TAL13	*Turdus albicollis nhaeozrvus* Cabanis, 1849	Museu Paraense Emilio Goeldi	MPEG 65655 (T8206)	AMANA 126	Brazil	Pará. Itaituba FLONA Amará Maranhense	-2.35242	-57.475	INGROUP	Tissue	SAMN12984441
TNU2	*Turdus nudigenis estimus* Todd, 1931	Museu Paraense Emilio Goeldi	MPEG 69976 (T10951)	MAR 009	Brazil	Pará, Marabá	-5,35	-49,11778	INGROUP	Tissue	SAMN12984442
TNU1	*Turdus nudirostris estimus* Todd. 1931	Museu Paraense Emilio Goeldi	MPEG 61072 (T4289)	PEMA 065	Brazil	Pará. Monte Alegre Parque Estadual Monte Alegre Arouche	-2.02447	-54.20939	INGROUP	Tissue	SAMN12984443
TLEU5	*Turdus leucomelas albiventer* Snix. 1824	Divisão de Aves do Museu de Zoologia da Universidade Estadual de Feira de Santan	DAMZUFS D.A 00062		Brazil	Bahia. Morro do Chanéu	-11.5825	-41.12	INGROUP	Tissue	SAMN12984444
TRUF10	*Turdus ruficrentris iuensis* (Cory, 1916)	Divisão de Aves do Museu de Zoologia da Universidade Estadual de Feira de Santan	DAMZUFS D.A 00926		Brazil	Bahia, Andaraí Marimbus	-12,7699	-41,31567	INGROUP	Tissue	SAMN12984445
TRUF1	*Turdus ruficrentris iuensis* (Corv. 1916)	Museu Paraense Emilio Goeldi	MPEG T10715 (LZUFPI 091	CAS186	Brazil	Piaui. Castelo do Piaui Fazenda Bonito	-5,30028	-41,53306	INGROUP	Tissue	SAMN12984446
TSCZ3	*Turdus sanchezorum* O'Neill et al., 2011	Museu Paraense Emilio Goeldi	MPEG 73567 (T16152)	MAD 333	Brazil	Amazonas, Manicoré, Colares margem leste Rio Madeira	-5,51803	-60,83372	INGROUP	Tissue	SAMN12984447
TSCZ1	*Turdus sanchezorum* O'Neill et al., 2011	Museu Paraense Emilio Goeldi	MPEG 63654 (T6043)	UFAC 1286	Brazil	Acre. Rio Branco Estrada do Ouinadá. Fazenda São Raimundo	-9.95897	-67.77256	INGROUP	Tissue	SAMN12984448
THX5	*Turdus hauwelli* Lawrence. 1869	Museu Paraense Emilio Goeldi	T17420	AMZ 537	Brazil	Mato Grosso. Nova Bandeirantes maruem direita Rio Juruena Fazenda Gerino	-10.3825	-58.32667	INGROUP	Tissue	SAMN12984449
U4169	*Turdus grayi linnaei* A. R. Phillips, 1966	Burke Museum	UWBM 101193	BTS 08 254	Mexico	Chiapas, Arriaga; small finca ouside of town	16.2083	-93.9332	INGROUP	Tissue	SAMN12984450
THX1	*Turdus hauwelli* Lawrence. 1869	Museu Paraense Emilio Goeldi	MPEG 61383 (T29811)	UFAC 803	Brazil	Acre, Rio Branco Transacreana AC090 km 70 Ramal Jurinal km 11	-9.90058	-68.47558	INGROUP	Tissue	SAMN12984451
TIG13	*Turdus ignobilis debilis* Hellmayr, 1902	Louisiana State University Museum of Natural Science	LSUMZ 7255	2473	Peru	Loreto, Department Isla Pasto Rio Amazonas opposite Aysana ca 80 km BE Iquitos	-3.76861	-73.28032	INGROUP	Tissue	SAMN12984452
TIG3	*Turdus ignobilis arthuri* (Chubb. 1914)	Museu Paraense Emilio Goeldi	MPEG 66844 (T9449)	ORX 034	Brazil	Pará. Oriximina Lago Sanucua Comunidade Casinha	1.76589	-56.22681	INGROUP	Tissue	SAMN12984453
TFU13	*Turdus flavines* Vieillot, 1818	Louisiana State University Museum of Natural Science	LSUMZ 69373	2403	Trinidad and Tobago	St. Georne Countv	10.725	-61.30667	INGROUP	Tissue	SAMN12984454
TFU1	*Turdus fumigatus fumigatus* M. H. K. Lichtenstein, 1823	Museu Paraense Emilio Goeldi	MPEG 61065 (T4292)	PEMA 069	Brazil	Pará, Monte Alegre Parque Estadual Monte Alegre Arouche	-2.02447	-54.20939	INGROUP	Tissue	SAMN12984455
TFL5	*Turdus flavines flavines* Vieillot, 1818	Laboratório de Genética e Evolução Molecular de Aves	LGEMA 16507		Brazil	São Paulo. Estação Ecológica de Boracéia Biritiba Mirim	-23.6555	-45.89082	INGROUP	Tissue	SAMN12984456
TFL2	*Turdus flavipes polionota* (Sharpe, 1902)	Divisão de Aves do Museu de Zoologia da Universidade Estadual de Feira de Santan	DAMZUFS D.A 00908		Brazil	Bahia Santa Teresinha Serra da Jibóia	-12,8603	-39,47375	INGROUP	Tissue	SAMN12984457
TLAW4	*Turdus lawrencii* Coues. 1880	Museu Paraense Emilio Goeldi	MPEG 67590 (T102511)	TLP(A) 108	Brazil	Mato Grosso, Paranaita maruem esauerda Rio Paranaita Fazenda Alianca	-9.665	-56.47639	INGROUP	Tissue	SAMN12984458
TLAW3	*Turdus lawrencii* Coues. 1880	Museu Paraense Emilio Goeldi	MPEG 70045 (T124621	JUR 051	Brazil	Acre. Feiió Rio Jurunari maruem esauerda Novo Oriente	-8.22142	-69.85517	INGROUP	Tissue	SAMN12984459
U4303	*Turdus merula merula* Linnaeus, 1758	Louisiana State University Museum of Natural Science	LSUMZ 12226		Sweden	Oland Ottenby Bird Observatory	56.2	16.4	INGROUP	Tissue	SAMN12984460
U4316	*Turdus nudigenis nudigenis* Lafresnave. 1848	Louisiana State University Museum of Natural Science	LSUMZ 69453(T7		Trinidad and Tobago	St. Georne Countv. Arinv Valley L'Oranee Estate	10.6862	-61.23417	INGROUP	Tissue	SAMN12984461
U1097	*Oenanthe oenanthe* (Linnaeus, 1758)	Naturhistoriska riksmuseet, Stockholm	NRM 2004-6483		Sweden	Arlanda	59,65	17.9	OUTGROUP	Tissue	SAMN12984462
GFB998	*Catharus aracilirostris* Salvin. 1865	American Museum of Natural Historv	AMNH DOT 3660		Costa Rica	3KM NORTH OF VILLA MILLS-LA GEORGINA 3000 METERS	9.36	83.42	OUTGROUP	Tissue	SAMN12984463
U3456	*Geokichla dumasi isiaeri* Rothschild. 1899	Zoological Museum, Universitv of Copenhagen	ZMUC 148346		Indonesia	Ceram	-4.40625	131.32135	OUTGROUP	Tissue	SAMN12984464
Bali	*Zoothera dauma horsfieldi* Latham, 1790	Department of Biology and Environmental Science, University of Gothenburg	DZUG 1136		Indonesia	Bali	-8.7	115.2	OUTGROUP	Tissue	SAMN12984465
BTC580	*Cichoa viridis* Hodason. 1836	American Museum of Natural Historv	AMNH DOT 12281	RTC580	Vietnam	Ouana Nam. Tra Mv District. Nuoc Linh Ranue	15.0725	107.97	OUTGROUP	Tissue	SAMN12984466
U4148	*Ridgwayia pinicola* P. L. Sclater, 1859	Burke Museum	UWBM 104375		Mexico		28,45	-108,1	OUTGROUP	Tissue	SAMN12984467
U3572 (DOT6948	*Turdus swalesi* Wetmore. 1927	American Museum of Natural Historv	AMNH DOT6948	NKK 1013	Dominican Republic	Prov. Independencia. Parque Nacional Sierra de Baoruco. Zanoten. Saw Mill Clearing. elev 1500	18.7357	-70.16265	INGROUP	Tissue	SAMN12984468
U4053	*Turdus rubrocanus* G. R. Grav. 1846	South Western Forestry Universitv. Kunming	SWFU05041		China	Lianhua Mts. Jiunzsi	27.1365	113.86507	INGROUP	Tissue	SAMN12984469
U4054	*Turdus hortulorum* P. L. Sclater, 1863	South Western Forestry Universitv	SWFU06034		China	Yihuang, Jiangxi	27.6128	116.22213	INGROUP	Tissue	SAMN12984470
U4178	*Psochocichla litsitsirupa* A. Smith. 1836	Burke Museum	UWBM 95229	GAV 1147	South Africa	Northwest Province. Vrotershoon. Molono Reserve	-25.7946	22.894737	INGROUP	Tissue	SAMN12984471
U4308	*Turdus migratorius phillipsi* Banas, 1915	Louisiana State University Museum of Natural Science	LSUMZ 83104		United States of America	New Mexico, JEMEZ SPRINGS	35.7686	-106.6923	INGROUP	Tissue	SAMN12984472
U4280	*Turdus chrysolaus* Temminck, 1832	Louisiana State University Museum of Natural Science	LSUMZ 16992		Japan	Nagano Prefecture, Nobeyama	35.9572	135.47493	INGROUP	Tissue	SAMN12984473
U4301	*Turdus merula merula* Linnaeus, 1758	Louisiana State University Museum of Natural Science	LSUMZ 13474		Germanv	Schelovia-Holstein, Helmeland	54.1803	7.8889444	INGROUP	Tissue	SAMN12984474
U4294	*Turdus iliacus iliacus* Linnaeus, 1766	Louisiana State University Museum of Natural Science	LSUMZ 31191		Russia	Belarus: Liahavitzi Raion Tuhawiczi	52,59	25,58	INGROUP	Tissue	SAMN12984475
GNM-Av.ex 7455	*Turdus fumigatus* M. H. K. Lichtenstein. 1823	Göteborg Naturhistoriska Museum – Exotic Collection.	GNM-Av.ex 7455		Ecuador		-2.07335	-76.72621	INGROUP	TocPads	SAMN12984476
GNM5775	*Turdus eunomus* Temminck, 1831	Göteborg Naturhistoriska Museum	GNM5775		Russia	Moneron Island	46,2528	141.23667	INGROUP	TocPads	SAMN12984477
GNM5778	*Turdus obscurus* J. F. Gmelin, 1789	Göteborg Naturhistoriska Museum	GNM5778		Russia	Moneron Island	46,2528	141.23667	INGROUP	TocPads	SAMN12984478
GNM6270	*Turdus hortulorum* P. L. Sclater. 1863	Göteborg Naturhistoriska Museum	GNM6270		China	Jianasu	32.1879	119.42584	INGROUP	TocPads	SAMN12984479
GNM5292	*Turdus iliacus* Linnaeus, 1766	Göteborg Naturhistoriska Museum	GNM5292		Iceland		66,4283	-17,33834	INGROUP	TocPads	SAMN12984480
U3649	*Turdus aurantius* J. F. Gmelin. 1789	American Museum of Natural Historv	AMNH 819420	163	Jamaica	St. Catherine	18.0392	-77.05523	INGROUP	TocPads	SAMN12984481
U3599	*Turdus lherminieri dominicensis* (Lawrence, 1880)	American Museum of Natural Historv	AMNH- SKIN 503684		West Indies	Dominica Island, Limbrevre	15.3999	-61.35965	INGROUP	TocPads	SAMN12984482
GNM-Av.su 172	*Turdus viscivorus* Linnaeus, 1758	Göteborg Naturhistoriska Museum	GNM-Av.su 172		Sweden		60.1282	-18.6435	INGROUP	TocPads	SAMN12984483
GNM-Av.ex 6245	*Turdus nallidus* J. F. Gmelin. 1789	Göteborg Naturhistoriska Museum – Exotic Collection.	GNM-Av.ex 6245		China	Jianasu	46.2528	141.23667	INGROUP	TocPads	SAMN12984484
GNM7449	*Turdus fuscater* Lafresnaye and d'Orbiany, 1837	Göteborg Naturhistoriska Museum – Exotic Collection.	GNM-Av.ex 7449		Ecuador		-0,3772	-78,14076	INGROUP	TocPads	SAMN12984485
GNM8238	*Turdus viscivorus* Linnaeus, 1758	Göteborg Naturhistoriska Museum	GNM-Av.su 8238		Sweden		60.1282	-18.6435	INGROUP	TocPads	SAMN12984486
GNM8762	*Turdus iliacus* Linnaeus, 1766	Göteborg Naturhistoriska Museum	GNM-Av.su 8762		Sweden	Västergötland	57,7	12,2	INGROUP	TocPads	SAMN12984487
U1774	*Turdus merula* Linnaeus, 1758	Department of Biology and Environmental Science, University of Gothenburg	DZUG 1774		Tunisia	Halk el Menzel, Herqla	35.9343	10.506036	INGROUP	TocPads	SAMN12984488
GNM10084	*Turdus serranus* Tschudi, 1844	Göteborg Naturhistoriska Museum – Exotic Collection.	GNM-Av.ex 10084		Ecuador		-1.04433	-79.82687	INGROUP	TocPads	SAMN12984489
GNM6136	*Turdus merula cabrerae* Hartert, 1901	Göteborg Naturhistoriska Museum – Exotic Collection.	GNM-Av.ex 6136		Spain	Canary Is., Tenerife	28,1675	-16,63571	INGROUP	TocPads	SAMN12984490
GNM1291	*Turdus ignobilis* P. L. Sclater. 1858	Göteborg Naturhistoriska Museum – Exotic Collection.	GNM-Av.ex 1291		Ecuador		0.39455	-78.01406	INGROUP	TocPads	SAMN12984491
GNM5706	*Turdus cardis* Temminck, 1831	Göteborg Naturhistoriska Museum – Exotic Collection.	GNM-Av.ex 5706		Russia		46,2528	141.23667	INGROUP	TocPads	SAMN12984492
GNM11676	*Turdus olivaceus abyssinicus* J. F. Gmelin, 1789	Göteborg Naturhistoriska Museum – Exotic Collection.	GNM-Av.ex 11676		Ethiopia		9.145	40.489672	INGROUP	TocPads	SAMN12984493
GNM780	*Turdus iliacus* Linnaeus. 1766	Göteborg Naturhistoriska Museum	GNM-Av.su 780		Sweden	Lanoland	68.141	26.868111	INGROUP	TocPads	SAMN12984494
GNM8584	*Turdus naumanni* Temminck, 1820	Göteborg Naturhistoriska Museum – Exotic Collection.	GNM-Av.ex 8584		China		33,0039	118,76323	INGROUP	TocPads	SAMN12984495

LSUMZ 1330

Table S2 List of additional loci used, including code or locus name, description, location in the chromosome and source when information is available.

Number	code/locus	description	Chomossome	Source
1	24813		1	Backström et al., 2008
2	26698	Histone-binding protein RBBP7 (retinoblastoma-binding protein 7) (RBBP-7) (retinoblastoma-binding protein p46). (Source:U	1	Backström et al., 2008
3	27331		1	Backström et al., 2008
4	23989	tumour differentially expressed 2 (Source:RefSeq_peptide; Acc:NP_001026245)	3	Backström et al., 2008
5	17483	High mobility group protein B2 (high mobility group protein 2) (HMG- 2) (Source:Uniprot/SWISSPROT; Acc:P26584)	4	Backström et al., 2008
6	25149	Carboxypeptidase Z precursor (EC 3.4.17.-) (CPZ) (cCPZ) (Source:Uniprot/SWISSPROT; Acc:Q8QGP3)	4	Backström et al., 2008
7	15724	acyl-coenzyme A dehydrogenase, short/branched chain (Source:RefSeq_peptide; Acc:NP_001026411)	6	Backström et al., 2008
8	18142	proteasome (prosome, macropain) 26S subunit, non-ATPase, 14 (Source:RefSeq_peptide; Acc:NP_001026427)	7	Backström et al., 2008
9	6419	adenosine deaminase-like (Source:RefSeq_peptide; Acc:NP_001025718)	10	Backström et al., 2008
10	3862	WD repeat protein 24 (Source:Uniprot/SWISSPROT; Acc:Q5ZMV9)	14	Backström et al., 2008
11	1658	Shwachman–Bodian–Diamond syndrome (Source:RefSeq_peptide; Acc:NP_001006211)	19	Backström et al., 2008
12	8235	Hypothetical protein (Source:Uniprot/SPTREMBL; Acc:Q5ZKN8)	unplaced Scaffold	Backström et al., 2008
13	4550	not in Ensembl database	-	Backström et al., 2008
14	VLDLR7	very low density lipoprotein receptor	Z	Backström et al., 2008
15	BRM12	SMARCA2 SWI/SNF related, matrix associated, actin dependent regulator of chromatin, subfamily a, member 2	Z	Backström et al., 2008
16	13403	proteasome (prosome, macropain) 26S subunit, ATPase, 2 (Source:RefSeq_peptide; Acc:NP_001006225)	1	Backström et al., 2008
17	21652	L-lactate dehydrogenase B chain (EC 1.1.1.27) (LDH-B). (Source:Uniprot/SWISSPROT; Acc:P00337)	1	Backström et al., 2008
18	10005		2	Backström et al., 2008
19	25969		2	Backström et al., 2008
20	13093		3	Backström et al., 2008
21	9949		4	Backström et al., 2008
22	20207	Hypothetical protein (Source:Uniprot/SPTREMBL; Acc:Q5ZJ03)	5	Backström et al., 2008
23	3978	RasGEF domain family, member 1 A (Source:RefSeq_peptide; Acc:NP_001026390)	6	Backström et al., 2008
24	4557	acyl-coenzyme A dehydrogenase, long chain (Source:RefSeq_peptide; Acc:NP_001006511)	7	Backström et al., 2008
25	3399	Pleckstrin homology domain-containing family B member 2 (Evectin-2) (Source: Uniprot/SWISSPROT; Acc:Q5F3S2)	9	Backström et al., 2008
26	13907		9	Backström et al., 2008
27	16934	Selenoprotein T precursor (Source:Uniprot/SWISSPROT; Acc:Q5ZJN8)	9	Backström et al., 2008
28	13336	eukaryotic translation initiation factor 3, subunit 1 alpha, 35 kDa (Source:RefSeq_peptide; Acc:NP_001012789)	10	Backström et al., 2008
29	1304	Casein kinase II subunit alpha' (EC 2.7.11.1) (CK II) (Source:Uniprot/SWISSPROT; Acc:P21869)	11	Backström et al., 2008
30	12260	dihydropyrimidinase-like 3 (Source:RefSeq_peptide; Acc:NP_989824)	13	Backström et al., 2008
31	6938		14	Backström et al., 2008
32	2108		15	Backström et al., 2008
33	12619	Pescadillo homologue 1 (Source:Uniprot/SWISSPROT; Acc:O00541)	15	Backström et al., 2008
34	9663		19	Backström et al., 2008
35	7793	Phosphopantothenate–cysteine ligase (EC 6.3.2.5) (phosphopantothenoylcysteine synthetase) (PPC synthetase) (Source:Unip	21	Backström et al., 2008
36	504	hypothetical protein LOC418842 (Source:RefSeq_peptide; Acc:NP_001006270)	23	Backström et al., 2008
37	2496		27	Backström et al., 2008
38	5915		28	Backström et al., 2008
39	14718	Superkiller viralicidic activity 2-like 2 (EC 3.6.1.-) (ATP-dependent helicase SKIV2L2) (Source:Uniprot/SWISSPROT; Acc:P42285	Z	Backström et al., 2008
40	12884	dihydrolipoamide dehydrogenase (Source:RefSeq_peptide; Acc:NP_001025898)	1	Backström et al., 2008
41	15506	Contactin-1 precursor (neural cell recognition molecule F11). (Source:Uniprot/SWISSPROT; Acc:P14781)	1	Backström et al., 2008
42	10623	vasoactive intestinal peptide receptor 2 (Source:RefSeq_peptide; Acc:NP_001014970)	2	Backström et al., 2008
43	22187	Myelin basic protein (MBP) (Source:Uniprot/SWISSPROT; Acc:P15720)	2	Backström et al., 2008
44	26472	Collagen alpha-1(XIV) chain precursor (undulin) (Source:Uniprot/SWISSPROT; Acc:P32018)	2	Backström et al., 2008
45	25442	ubiquitin-conjugating enzyme E2, J1 (UBC6 homologue, yeast) (Source:RefSeq_peptide; Acc:NP_990094)	3	Backström et al., 2008
46	17367	26S protease regulatory subunit 4 (P26s4) (proteasome 26S subunit ATPase 1) (Source:Uniprot/SWISSPROT; Acc:Q90732)	5	Backström et al., 2008
47	7248		8	Backström et al., 2008
48	17388	mago-nashi homologue, proliferation-associated (Source:RefSeq_peptide; Acc:NP_989656)	8	Backström et al., 2008
49	MC1R	melanocortin 1 receptor	11	Backström et al., 2008
50	ACA			Harvey, 2015
51	ACO1	aconitase 1, soluble	Z	Harvey, 2015
52	ALD	aldolase	no info	Harvey, 2015
53	ARNTL	aryl hydrocarbon receptor nuclear translocator like	no info	Harvey, 2015
54	BDNF	brain derived neurotrophic factor	5	Harvey, 2015
55	CALB1	calbindin 1	2	Harvey, 2015
56	CHC (CLTC)	clathrin heavy chain	19	Harvey, 2015
57	CLK	clock	no info	Harvey, 2015
58	CLOCK	clock circadian regulator.	4	Harvey, 2015
58	CLTCL1	clathrin heavy chain like 1.	22	Harvey, 2015
59	CMYC	v-myc avian myelocytomatosis viral oncogene homolog	2	Harvey, 2015
60	CSDE1	cold shock domain containing E1	26	Harvey, 2015
61	DCOH (PCBD1)	pterin-4 alpha-carbinolamine dehydratase 1	6	Harvey, 2015
62	CSNK1E	casein kinase 1 epsilon	1	Harvey, 2015
63	DDX5	DEAD-box helicase 5	Unplaced Scaffold	Harvey, 2015
64	EEF	eukaryotic translation elongation factor		Harvey, 2015
65	EGR1	early growth response 1	13	Harvey, 2015
66	EIF5	eukaryotic translation initiation factor 5	5	Harvey, 2015
67	ENO1	enolase 1, (alpha)	21	Harvey, 2015
68	GRIA2	glutamate ionotropic receptor AMPA type subunit 2	4	Harvey, 2015
69	HMG (HMGN4)	high mobility group nucleosomal binding domain 4	23	Harvey, 2015
70	HNRNPA2B1	heterogeneous nuclear ribonucleoprotein A2/B1	2	Harvey, 2015
71	HOXA	homeobox A cluster		Harvey, 2015
72	IRF1	interferon regulatory factor 1	13	Harvey, 2015
73	KCNQ5	potassium voltage-gated channel subfamily Q member 5	3	Harvey, 2015
74	MUSK	muscle, skeletal, receptor tyrosine kinase	Z	Harvey, 2015
75	NAA60 (NAT15)	N(alpha)-acetyltransferase 60, NatF catalytic subunit	14	Harvey, 2015
76	NGF	nerve growth factor	26	Harvey, 2015
77	NTF3	neurotrophin 3	1	Harvey, 2015
78	ODC1	ornithine decarboxylase 1	3	Harvey, 2015
79	PARK7	Parkinson disease (autosomal recessive, early onset) 7	21	Harvey, 2015
80	PDE6B	phosphodiesterase 6B	Z	Harvey, 2015
81	PER2	period circadian clock 2	9	Harvey, 2015
82	PPP2CB	protein phosphatase 2 catalytic subunit beta	4	Harvey, 2015
83	PSMA2	proteasome subunit alpha 2	2	Harvey, 2015
83	PSMA	proteasome		Harvey, 2015
84	RAG1	recombination activating 1	5	Harvey, 2015
85	RAG2	recombination activating 2	5	Harvey, 2015
86	RAPGEF1	Rap guanine nucleotide exchange factor 1	17	Harvey, 2015
87	RHOD	ras homolog family member D	Unplaced Scaffold	Harvey, 2015

88	SBDS	SBDS ribosome assembly guanine nucleotide exchange factor	19	Harvey, 2015
89	SEPT2	septin 2	9	Harvey, 2015
90	SOMA			Harvey, 2015
91	SUCLG1	succinate-CoA ligase alpha subunit	4	Harvey, 2015
92	TXNDC12	thioredoxin domain containing 12	8	Harvey, 2015
93	VDAC2	voltage dependent anion channel 2	6	Harvey, 2015
94	VIM	vimentin	2	Harvey, 2015
95	ALDOB	aldolase, fructose-bisphosphate B	Z	Harvey, 2015

Table S3. Quality control after trimming using the PHYLUCE pipeline.

samples	reads	total base pairs	mean length	95 CI length	minimum	maximum	median
U2338	1012978	249219091	246,0261635	0,065984449	40	301	272
U3899	723404	176746449	244,3260599	0,079944499	40	301	271
U4155	1287700	311751988	242,0998587	0,059042297	40	301	266
U4159	899776	224353255	249,3434533	0,069347335	40	301	277
U4162	949773	236893800	249,4214933	0,066665403	40	301	275
U4163	1324780	319777258	241,3814052	0,057819107	40	301	263
U4164	757123	183335173	242,1471452	0,076157202	40	301	264
U4166	1179423	292508760	248,0100524	0,06174044	40	301	276
U4168	1366917	343577070	251,3518158	0,055260561	40	301	279
U4170	1573272	385549507	245,062206	0,052688229	40	301	271
U4172	1123582	271886712	241,9820823	0,062141555	40	301	264
U4176	1225960	297311565	242,5132672	0,060936417	40	301	267
U4177	1410551	356772030	252,9309681	0,053420887	40	301	280
U4179	2036667	512876677	251,8215678	0,045834905	40	301	281
U4185	1004514	249679575	248,5575861	0,067771511	40	301	278
U4187	129766	31861427	245,5298537	0,189743909	40	301	273
U4188	966152	237380702	245,697056	0,067969219	40	301	272
U4189	627462	157289243	250,6753285	0,082290656	40	301	278
U4192	789627	193558595	245,1266167	0,078486925	40	301	275
U4273	1767776	447079437	252,905027	0,047753256	40	301	280
U4279	876435	214418802	244,6488353	0,070362741	40	301	268
U4281	1080731	270373140	250,1761678	0,061467404	40	301	276
U4285	1202545	299028546	248,663082	0,058614511	40	301	275
U4287	1954004	491557894	251,5644257	0,04734589	40	301	282
U4292	955476	234938942	245,8868062	0,067068208	40	301	270
U4297	1068930	266340548	249,1655656	0,064316475	40	301	277
U4299	1738881	437056955	251,3437981	0,04609414	40	301	274
U4305	656016	155954409	237,7295813	0,075634587	40	301	250
U4309	995238	249848514	251,0439855	0,066259004	40	301	281
U4312	740502	185157722	250,0435137	0,077636681	40	301	280
U4314	1067878	269002783	251,9040405	0,062940745	40	301	281
U4315	852825	207899878	243,7778888	0,075507931	40	301	272
U4317	1519039	384864087	253,3602409	0,051862643	40	301	282
U4319	1253453	312132253	249,0179153	0,057395171	40	301	275
U4320	658636	156238357	237,2150277	0,083116438	40	301	257
U4321	1068882	266691344	249,5049444	0,064832551	40	301	279
U4322	1555790	381173729	245,0033289	0,055951634	40	301	274
U4325	1014928	243430082	239,8496071	0,0665418	40	301	261
U4329	1002038	246944943	246,4426928	0,066288071	40	301	272
U4331	1056110	257277409	243,6085341	0,064296491	40	301	267
U4332	749929	177747541	237,0191591	0,079481137	40	301	258
U4334	738961	183623528	248,4887944	0,076282947	40	301	275
U4336	1132500	279425814	246,7336106	0,061010828	40	301	271
U4337	661535	151643152	229,2292199	0,07972637	40	301	241
U4338	1128316	284932377	252,5288811	0,061412377	40	301	283
U4339	1116113	276157009	247,4274639	0,06213276	40	301	273
U4340	1108044	277731444	250,6501944	0,062876366	40	301	280
U4345	1089228	261793754	240,3479841	0,063607622	40	301	262
Bali	972331	240064047	246,8953957	0,075113069	40	301	288
BTC580	1015780	251742031	247,8312538	0,072659513	40	301	289

U3572 (DOT	844655	205482219	243,2735484	0,079833087	40	301	278
GFB998	783593	194040288	247,6289196	0,084171305	40	301	291
TAL13	660694	160566677	243,0272971	0,091345092	40	301	279
TAL24	662921	159339921	240,3603461	0,094269565	40	301	278
TAM2	1333741	327995771	245,9216377	0,062408152	40	301	282
TAM6	554234	132696165	239,4226356	0,103640966	40	301	276
TFL2	999161	245756812	245,9631751	0,073415753	40	301	283
TFL5	1291805	317845459	246,0475528	0,064492984	40	301	285
TFU1	1127747	271945895	241,140872	0,071772996	40	301	279
TFU13	837988	206955122	246,9666893	0,080893935	40	301	288
THX1	771404	186454885	241,7084757	0,085309501	40	301	278
THX5	1039185	253021311	243,4805266	0,073142114	40	301	281
TIG13	1429444	353707763	247,4442951	0,061253086	40	301	289
TIG3	1187264	293311726	247,0484458	0,066813717	40	301	286
TLAW3	1216394	300832662	247,3151479	0,066392139	40	301	288
TLAW4	1176451	292581023	248,6980104	0,06701537	40	301	290
TLEU5	953831	232058063	243,2905441	0,073135996	40	301	275
TNU1	1171769	286225526	244,267877	0,068899959	40	301	282
TNU2	1300434	319696378	245,8382186	0,064571004	40	301	284
TRUF1	1277649	314908687	246,4751172	0,065082313	40	301	286
TRUF10	898326	220267968	245,1982554	0,078477401	40	301	285
TSCZ1	972815	239772819	246,4731927	0,075236152	40	301	287
TSCZ3	1290572	318869578	247,0761631	0,064437429	40	301	288
U1097	1015709	248193955	244,3553764	0,074707565	40	301	284
U1098	1369418	340283669	248,4878021	0,061801585	40	301	289
U3456	899380	222090348	246,9371656	0,078348176	40	301	289
U4053	904782	225849404	249,6174813	0,074640473	40	301	289
U4054	1011573	250525131	247,6589737	0,072591434	40	301	287
U4148	1031444	255451986	247,6644258	0,072275341	40	301	289
U4156	993954	245212052	246,7036221	0,07212532	40	301	284
U4169	914091	223217448	244,1960899	0,07755667	40	301	283
U4175	977089	239697091	245,3175617	0,072925125	40	301	280
U4178	1455722	358442686	246,2301772	0,061471731	40	301	287
U4190	988804	244917158	247,6902986	0,073643052	40	301	289
U4194	1200273	295761379	246,4117572	0,066907662	40	301	286
U4275	1097999	268805266	244,8137621	0,070054603	40	301	282
U4280	663484	158895714	239,4868814	0,089020859	40	301	269
U4282	1214791	291814350	240,2177412	0,069624553	40	301	278
U4294	1208730	294713244	243,8205753	0,064532772	40	301	274
U4301	773100	179627165	232,346611	0,090192909	40	301	266
U4303	1159540	284384082	245,255948	0,068752336	40	301	284
U4308	684353	166663298	243,5341089	0,090811918	40	301	283
U4316	797714	192346148	241,1216902	0,085506322	40	301	279
U4335	1165730	281942185	241,8589082	0,068763556	40	301	277
U4352	864871	214873353	248,445552	0,078630804	40	301	290
GNM10084	1322336	135556747	102,5130882	0,035593745	40	251	95
GNM11291	1202387	125566144	104,4307232	0,036002436	40	251	98
GNM11676	14686	2416075	164,515525	0,564243961	40	251	161
GNM172	937721	107982291	115,1539648	0,041604034	40	251	111
GNM5292	720579	86542147	120,1008453	0,049512035	40	251	116
GNM5706	440600	56814946	128,9490377	0,067567384	40	251	125
GNM5775	871031	106943615	122,7781962	0,045441672	40	251	119
GNM5778	603851	74314547	123,0676889	0,056159831	40	251	119

GNM6136	1195342	144383360	120,7883267	0,038238317	40	251	117
GNM6245	1232489	158432632	128,5468933	0,039926145	40	251	126
GNM6270	1257352	142359579	113,2217382	0,035974002	40	251	110
GNM7449	1035648	113034325	109,1435748	0,040692702	40	251	103
GNM7455	1053628	127802809	121,297848	0,047917574	40	251	114
GNM780	913165	115588688	126,5802872	0,046651912	40	251	123
GNM8238	1878746	304161769	161,8961632	0,035690294	40	251	162
GNM8584	1312628	169481538	129,116199	0,038678763	40	251	126
GNM8762	1205711	257416626	213,4977835	0,041426022	40	251	228
U1774	1780967	374256176	210,1421172	0,035183842	40	251	224
U3599	1440180	177049843	122,9359129	0,03817315	40	251	118
U3649	2062348	267366087	129,6415964	0,032526451	40	251	126

Table S4. Quality control after assembly using the PHYLUCE pipeline.

Sample	Reads	Base pairs	Averange length	standard error length	Minimum le	Maximum le	Median leng	Contigs > 1kb	Quality Control	Source	Sequencer	Core Facility
GNM10084	3456	993221	287,3903356	3,627150127	224	10795	247	10	After Assembly_Trinity	ToePad	Miseq	SciLifeLab_Stockolm
GNM11291	4232	1218455	287,9146975	2,855316648	224	10795	250	8	After Assembly_Trinity	ToePad	Miseq	SciLifeLab_Stockolm
GNM11676	708	189219	267,2584746	15,08393687	224	10795	240	2	After Assembly_Trinity	ToePad	Miseq	SciLifeLab_Stockolm
GNM172	5976	1863198	311,7801205	2,705279995	224	10771	265	50	After Assembly_Trinity	ToePad	Miseq	SciLifeLab_Stockolm
GNM5292	4633	1438899	310,5760846	3,167926192	224	10795	260	44	After Assembly_Trinity	ToePad	Miseq	SciLifeLab_Stockolm
GNM5706	5024	1459656	290,5366242	2,544985302	224	10795	250	16	After Assembly_Trinity	ToePad	Miseq	SciLifeLab_Stockolm
GNM5775	7899	2362345	299,0688695	1,914137655	224	10795	257	40	After Assembly_Trinity	ToePad	Miseq	SciLifeLab_Stockolm
GNM5778	4097	1238535	302,3029046	3,309825804	224	10795	254	23	After Assembly_Trinity	ToePad	Miseq	SciLifeLab_Stockolm
GNM6136	11113	3438196	309,3850445	1,969173433	224	10795	263	72	After Assembly_Trinity	ToePad	Miseq	SciLifeLab_Stockolm
GNM6245	16561	4938301	298,1885756	1,137128474	224	10795	260	58	After Assembly_Trinity	ToePad	Miseq	SciLifeLab_Stockolm
GNM6270	7435	2280375	306,7081372	2,075498566	224	10795	266	40	After Assembly_Trinity	ToePad	Miseq	SciLifeLab_Stockolm
GNM7449	4755	1378343	289,8723449	2,638871818	224	10795	252	9	After Assembly_Trinity	ToePad	Miseq	SciLifeLab_Stockolm
GNM7455	12066	3495999	289,7396818	1,416704926	224	10795	248	59	After Assembly_Trinity	ToePad	Miseq	SciLifeLab_Stockolm
GNM780	6558	2083571	317,7143946	3,041325311	224	10795	253	77	After Assembly_Trinity	ToePad	Miseq	SciLifeLab_Stockolm
GNM8238	72422	21270952	293,7084311	1,035346498	224	31561	249	401	After Assembly_Trinity	ToePad	Miseq	SciLifeLab_Stockolm
GNM8584	17006	4996536	293,8101846	0,96741766	224	10795	259	25	After Assembly_Trinity	ToePad	Miseq	SciLifeLab_Stockolm
GNM8762	111014	31409732	282,9348731	0,452416207	224	10795	244	580	After Assembly_Trinity	ToePad	Miseq	SciLifeLab_Stockolm
U1774	181582	52046772	286,6295778	0,34003765	224	10795	247	791	After Assembly_Trinity	ToePad	Miseq	SciLifeLab_Stockolm
U3599	10319	3030288	293,6610137	1,609132539	224	10795	251	53	After Assembly_Trinity	ToePad	Miseq	SciLifeLab_Stockolm
U3649	34803	10034161	288,3131052	0,635076505	224	10771	253	94	After Assembly_Trinity	ToePad	Miseq	SciLifeLab_Stockolm
U2338	24384	10037572	411,6458333	1,812531763	224	10795	300	1846	After Assembly_Trinity	FreshTissue	Miseq	SciLifeLab_Upssala
U3899	19460	8556950	439,7199383	2,480551729	224	22411	306	1866	After Assembly_Trinity	FreshTissue	Miseq	SciLifeLab_Upssala
U4155	31974	12822211	401,0199224	1,52827837	224	10795	301	2177	After Assembly_Trinity	FreshTissue	Miseq	SciLifeLab_Upssala
U4159	20969	9413181	448,9093901	2,138687991	224	10795	315	2064	After Assembly_Trinity	FreshTissue	Miseq	SciLifeLab_Upssala
U4162	21186	9043093	426,8428679	1,832809718	224	10795	314	1412	After Assembly_Trinity	FreshTissue	Miseq	SciLifeLab_Upssala
U4163	38558	14985148	388,639141	1,292798834	224	10795	298	2143	After Assembly_Trinity	FreshTissue	Miseq	SciLifeLab_Upssala
U4164	19037	8250755	433,4062615	2,154075977	224	10795	308	1625	After Assembly_Trinity	FreshTissue	Miseq	SciLifeLab_Upssala
U4166	28268	12091318	427,7387152	1,677682695	224	10795	316	2116	After Assembly_Trinity	FreshTissue	Miseq	SciLifeLab_Upssala
U4168	30754	12790746	415,905118	1,520896727	224	10795	313	2024	After Assembly_Trinity	FreshTissue	Miseq	SciLifeLab_Upssala
U4170	35884	14195140	395,5841043	1,390655812	224	14874	303	2061	After Assembly_Trinity	FreshTissue	Miseq	SciLifeLab_Upssala
U4172	32346	12685670	392,1866691	1,375693841	224	10795	302	1738	After Assembly_Trinity	FreshTissue	Miseq	SciLifeLab_Upssala
U4176	30929	12645210	408,8463901	1,56323169	224	10795	305	2202	After Assembly_Trinity	FreshTissue	Miseq	SciLifeLab_Upssala
U4177	31012	12748900	411,0957049	1,450653098	224	10795	310	1954	After Assembly_Trinity	FreshTissue	Miseq	SciLifeLab_Upssala
U4179	37653	15384032	408,5738719	1,464648477	224	16715	309	2431	After Assembly_Trinity	FreshTissue	Miseq	SciLifeLab_Upssala
U4185	21076	9527634	452,0608275	2,264952649	224	10795	314	2214	After Assembly_Trinity	FreshTissue	Miseq	SciLifeLab_Upssala
U4187	5086	2684581	527,8373968	4,274614402	224	7448	405	321	After Assembly_Trinity	FreshTissue	Miseq	SciLifeLab_Upssala
U4188	25529	10572284	414,128403	1,741289087	224	10795	307	1850	After Assembly_Trinity	FreshTissue	Miseq	SciLifeLab_Upssala
U4189	15875	7287770	459,072126	2,430166276	224	10795	320	1572	After Assembly_Trinity	FreshTissue	Miseq	SciLifeLab_Upssala
U4192	16711	8095529	484,4431213	2,708794709	224	10795	320	2140	After Assembly_Trinity	FreshTissue	Miseq	SciLifeLab_Upssala
U4273	38783	15582737	401,7929763	1,247858497	224	10795	311	2180	After Assembly_Trinity	FreshTissue	Miseq	SciLifeLab_Upssala
U4279	23161	9691762	418,451794	1,903348859	224	10795	302	1832	After Assembly_Trinity	FreshTissue	Miseq	SciLifeLab_Upssala
U4281	31902	12596746	394,8575638	1,408450923	224	10795	307	1721	After Assembly_Trinity	FreshTissue	Miseq	SciLifeLab_Upssala
U4285	26770	10781203	402,7345163	1,565420908	224	10795	304	1536	After Assembly_Trinity	FreshTissue	Miseq	SciLifeLab_Upssala
U4287	34251	14545114	424,6624624	1,533151453	224	10795	312	2538	After Assembly_Trinity	FreshTissue	Miseq	SciLifeLab_Upssala
U4292	23385	9613101	411,0797947	1,724225214	224	10795	305	1555	After Assembly_Trinity	FreshTissue	Miseq	SciLifeLab_Upssala
U4297	26792	11336077	423,1142505	1,717226983	224	10795	313	2088	After Assembly_Trinity	FreshTissue	Miseq	SciLifeLab_Upssala
U4299	42021	14659312	348,8568097	0,941060265	224	10795	285	840	After Assembly_Trinity	FreshTissue	Miseq	SciLifeLab_Upssala
U4305	20347	7596095	373,3275176	1,558586568	224	10795	286	451	After Assembly_Trinity	FreshTissue	Miseq	SciLifeLab_Upssala
U4309	21303	9327226	437,8362672	2,165971512	224	10795	310	1987	After Assembly_Trinity	FreshTissue	Miseq	SciLifeLab_Upssala
U4312	18675	8440804	451,9841499	2,349710715	224	10795	315	1944	After Assembly_Trinity	FreshTissue	Miseq	SciLifeLab_Upssala
U4314	26471	11029044	416,6462922	1,673396199	224	10795	308	1910	After Assembly_Trinity	FreshTissue	Miseq	SciLifeLab_Upssala
U4315	19708	9114937	462,4993404	2,466906233	224	10795	313	2257	After Assembly_Trinity	FreshTissue	Miseq	SciLifeLab_Upssala
U4317	35523	13944510	392,5487712	1,322364258	224	10795	301	1989	After Assembly_Trinity	FreshTissue	Miseq	SciLifeLab_Upssala
U4319	30498	12319726	403,9519313	1,479933999	224	10795	305	1894	After Assembly_Trinity	FreshTissue	Miseq	SciLifeLab_Upssala
U4320	22411	8927665	398,3608496	1,753780622	224	10795	298	1293	After Assembly_Trinity	FreshTissue	Miseq	SciLifeLab_Upssala
U4321	23496	10197182	433,99651	1,921612904	224	10795	312	2076	After Assembly_Trinity	FreshTissue	Miseq	SciLifeLab_Upssala
U4322	27529	12474860	453,1534019	2,097418237	224	10795	312	2637	After Assembly_Trinity	FreshTissue	Miseq	SciLifeLab_Upssala
U4325	32769	12625182	385,2782203	1,410652051	224	10795	294	1789	After Assembly_Trinity	FreshTissue	Miseq	SciLifeLab_Upssala
U4329	29662	11729526	395,4394849	1,416402337	224	10795	306	1118	After Assembly_Trinity	FreshTissue	Miseq	SciLifeLab_Upssala
U4331	27751	11416246	411,3814277	1,712540609	224	10795	307	1834	After Assembly_Trinity	FreshTissue	Miseq	SciLifeLab_Upssala
U4332	21893	9002860	411,2209382	1,966595132	224	10795	297	1713	After Assembly_Trinity	FreshTissue	Miseq	SciLifeLab_Upssala
U4334	24285	9866532	406,2809141	1,801687626	224	11501	303	1533	After Assembly_Trinity	FreshTissue	Miseq	SciLifeLab_Upssala
U4336	30358	12064233	397,3988076	1,461011644	224	10795	302	1636	After Assembly_Trinity	FreshTissue	Miseq	SciLifeLab_Upssala
U4337	24210	8644012	357,0430401	1,166682931	224	10795	290	155	After Assembly_Trinity	FreshTissue	Miseq	SciLifeLab_Upssala
U4338	23074	10144471	439,6494323	2,11551047	224	18523	311	2159	After Assembly_Trinity	FreshTissue	Miseq	SciLifeLab_Upssala
U4339	29936	12282468	410,2908872	1,694325623	224	17622	308	1976	After Assembly_Trinity	FreshTissue	Miseq	SciLifeLab_Upssala
U4340	22547	10135478	449,5266776	2,175137154	224	10795	312	2295	After Assembly_Trinity	FreshTissue	Miseq	SciLifeLab_Upssala
U4345	32872	12463774	379,1608055	1,336019021	224	10795	296	1573	After Assembly_Trinity	FreshTissue	Miseq	SciLifeLab_Upssala
Bali	19992	9282736	464,322529	2,260311208	224	10795	323	2076	After Assembly_Trinity	FreshTissue	Miseq	SciLifeLab_Upssala
BTC580	19110	9078567	475,0689168	2,374200929	224	10795	327	2129	After Assembly_Trinity	FreshTissue	Miseq	SciLifeLab_Upssala
U3572 (DOT6948)	27214	11141108	409,388844	1,502948995	224	10795	313	1410	After Assembly_Trinity	FreshTissue	Miseq	SciLifeLab_Upssala
GFB998	17380	8351015	480,4956847	2,483969514	224	10795	333	2023	After Assembly_Trinity	FreshTissue	Miseq	SciLifeLab_Upssala
TAL13	19827	8901209	448,943814	2,151416413	224	10795	321	1818	After Assembly_Trinity	FreshTissue	Miseq	SciLifeLab_Upssala
TAL24	20083	9207645	458,4795598	2,379901208	224	13259	320	2009	After Assembly_Trinity	FreshTissue	Miseq	SciLifeLab_Upssala
TAM2	32825	13384564	407,7551866	1,394081637	224	10795	317	1694	After Assembly_Trinity	FreshTissue	Miseq	SciLifeLab_Upssala
TAM6	22039	9563624	433,9409229	1,935354047	224	10795	318	1763	After Assembly_Trinity	FreshTissue	Miseq	SciLifeLab_Upssala
TFL2	33305	13422179	403,0079267	1,352955472	224	10795	312	1818	After Assembly_Trinity	FreshTissue	Miseq	SciLifeLab_Upssala
TFL5	31819	13411644	421,4979729	1,562881799	224	10795	314	2306	After Assembly_Trinity	FreshTissue	Miseq	SciLifeLab_Upssala
TFU13	23017	10037061	436,0716427	1,905331934	224	10795	317	1952	After Assembly_Trinity	FreshTissue	Miseq	SciLifeLab_Upssala
TFU1	25193	11173237	443,5056166	1,927438462	224	10795	320	2216	After Assembly_Trinity	FreshTissue	Miseq	SciLifeLab_Upssala
THX1	21640	9456639	436,9981054	2,014737454	224	10795	315	1903	After Assembly_Trinity	FreshTissue	Miseq	SciLifeLab_Upssala
THX5	26699	11596004	434,3235327	1,84955501	224	10795	316	2136	After Assembly_Trinity	FreshTissue	Miseq	SciLifeLab_Upssala
TIG13	35298	14495927	410,6727577	1,437326697	224	13947	313	2268	After Assembly_Trinity	FreshTissue	Miseq	SciLifeLab_Upssala
TIG3	29587	12352666	417,5031602	1,562072715	224	10795	314	2076	After Assembly_Trinity	FreshTissue	Miseq	SciLifeLab_Upssala
TLAW3	30561	12884291	421,5925853	1,582360234	224	10795	314	2193	After Assembly_Trinity	FreshTissue	Miseq	SciLifeLab_Upssala
TLAW4	30823	12696877	411,9286572	1,427957044	224	10795	313	1831	After Assembly_Trinity	FreshTissue	Miseq	SciLifeLab_Upssala
TLEU5	30646	11967755	390,5160543	1,230950101	224	10795	313	834	After Assembly_Trinity	FreshTissue	Miseq	SciLifeLab_Upssala
TNU1	35064	14541909	414,7247604	1,412963629	224	13304	319	2166	After Assembly_Trinity	FreshTissue	Miseq	SciLifeLab_Upssala
TNU2	37560	15397727	409,9501331	1,278379828	224	10795	317	2155	After Assembly_Trinity	FreshTissue	Miseq	SciLifeLab_Upssala
TRUF10	23848	10480270	439,4611707	1,932059751	224	10795	315	2082	After Assembly_Trinity	FreshTissue	Miseq	SciLifeLab_Upssala
TRUF1	31292	12940479	413,5395309	1,477469716	224	10795	313	2065	After Assembly_Trinity	FreshTissue	Miseq	SciLifeLab_Upssala
TSCZ1	24883	10868201	436,7721336	1,840961643	224	10795	316	2071	After Assembly_Trinity	FreshTissue	Miseq	SciLifeLab_Upssala
TSCZ3	29815	12686094	425,4936777	1,792699626	224	14855	313	2250	After Assembly_Trinity	FreshTissue	Miseq	SciLifeLab_Upssala
U1097	21338	9895441	463,7473521	2,229534976	224	10795	321	2236	After Assembly_Trinity	FreshTissue	Miseq	SciLifeLab_Upssala
U1098	32293	13542836	419,3737342	1,6003874	224	16784	314	2224	After Assembly_Trinity	FreshTissue	Miseq	SciLifeLab_Upssala
U3456	16762	8081437	482,1284453	2,590558911	224	10795	328	2039	After Assembly_Trinity	FreshTissue	Miseq	SciLifeLab_Upssala
U4053	28110	11346541	403,6478477	1,522908902	224	15610	314	1370	After Assembly_Trinity	FreshTissue	Miseq	SciLifeLab_Upssala
U4054	29549	12199453	412,8550205	1,578162303	224	13091	313	1830	After Assembly_Trinity	FreshTissue	Miseq	SciLifeLab_Upssala
U4148	23501	10537972	448,4052594	1,992427221	224	10795	320	2117	After Assembly_Trinity	FreshTissue	Miseq	SciLifeLab_Upssala
U4156	29336	12123752	413,2721571	1,525539918	224	10795	313	1740	After Assembly_Trinity	FreshTissue	Miseq	SciLifeLab_Upssala
U4169	23071	10108999	438,1690867	2,008103332	224	13733	316	1985	After Assembly_Trinity	FreshTissue	Miseq	SciLifeLab_Upssala
U4175	29813	12055913	404,3844296	1,385141614	224	10795	315	1121	After Assembly_Trinity	FreshTissue	Miseq	SciLifeLab_Upssala

U4178	27323	12450022	455,6608718	2,18621926	224	19226	321	2457	After Assembly_Trinity	FreshTissue	Miseq	SciLifeLab_Upssala
U4190	24774	10863554	438,5062566	1,773225392	224	10795	323	1939	After Assembly_Trinity	FreshTissue	Miseq	SciLifeLab_Upssala
U4194	31133	13059120	419,4623069	1,683706287	224	17392	315	2187	After Assembly_Trinity	FreshTissue	Miseq	SciLifeLab_Upssala
U4275	27442	11628045	423,7316887	1,624657615	224	10795	316	1932	After Assembly_Trinity	FreshTissue	Miseq	SciLifeLab_Upssala
U4280	26386	10356986	392,5182294	1,34246928	224	10795	312	656	After Assembly_Trinity	FreshTissue	Miseq	SciLifeLab_Upssala
U4282	23322	11076678	474,9454592	2,315201092	224	10795	322	2486	After Assembly_Trinity	FreshTissue	Miseq	SciLifeLab_Upssala
U4294	36879	14387855	390,1367987	1,193038453	224	10795	311	1549	After Assembly_Trinity	FreshTissue	Miseq	SciLifeLab_Upssala
U4301	20966	9620042	458,8401221	2,389133012	224	16741	319	2121	After Assembly_Trinity	FreshTissue	Miseq	SciLifeLab_Upssala
U4303	31083	13168664	423,661294	1,685870941	224	18529	315	2274	After Assembly_Trinity	FreshTissue	Miseq	SciLifeLab_Upssala
U4308	21270	9375819	440,800141	2,027721393	224	10795	319	1800	After Assembly_Trinity	FreshTissue	Miseq	SciLifeLab_Upssala
U4316	23503	10262549	436,6484704	1,959544481	224	10795	315	2025	After Assembly_Trinity	FreshTissue	Miseq	SciLifeLab_Upssala
U4335	26100	11071576	424,1983142	1,755386819	224	13862	315	1735	After Assembly_Trinity	FreshTissue	Miseq	SciLifeLab_Upssala
U4352	17474	8319601	476,1131395	2,492831721	224	10795	326	2045	After Assembly_Trinity	FreshTissue	Miseq	SciLifeLab_Upssala

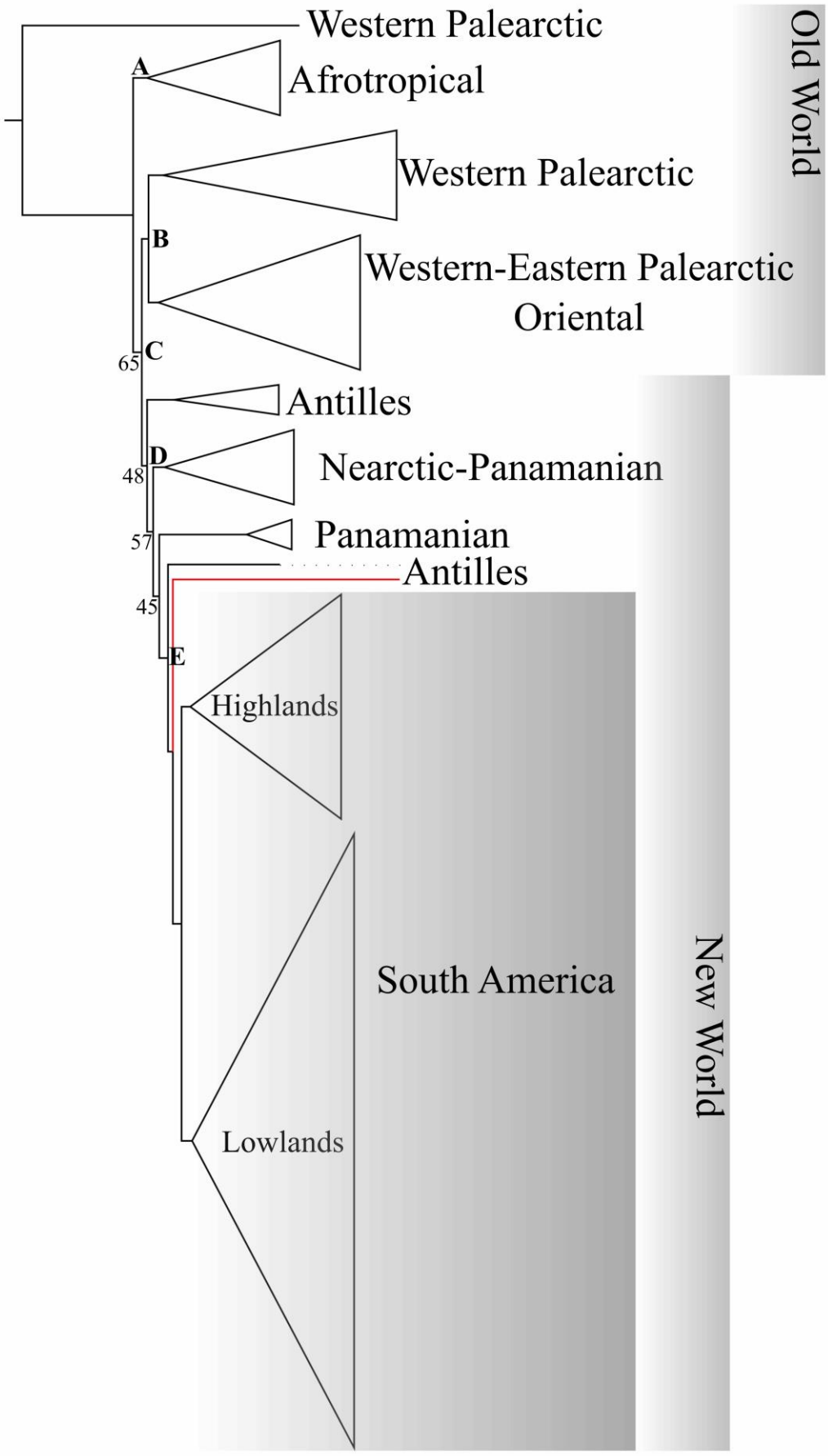
Western Palearctic
A
Afrotropical
Western Palearctic
B
Western-Eastern Palearctic
Oriental
65
C
Antilles
D
48
Nearctic-Panamanian
57
Panamanian
Antilles
45
E
Highlands
South America
Lowlands
Old World
New World

a) Voelker et al 2007

Turdus philomelos **(Palaearctic)**

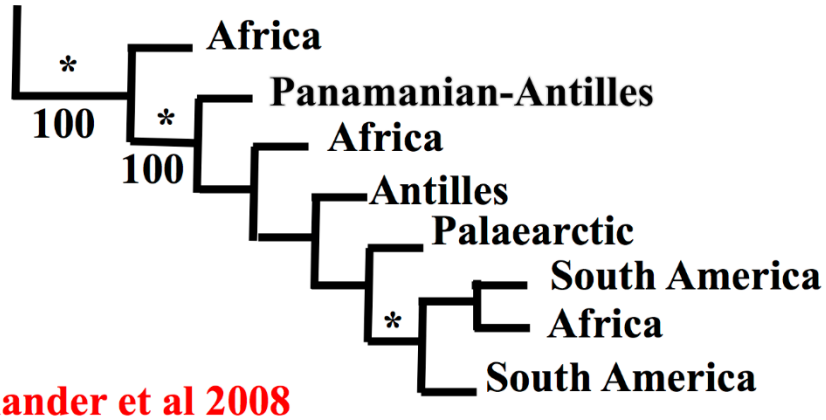

b) Nylander et al 2008

Turdus philomelos **(Palaearctic)**

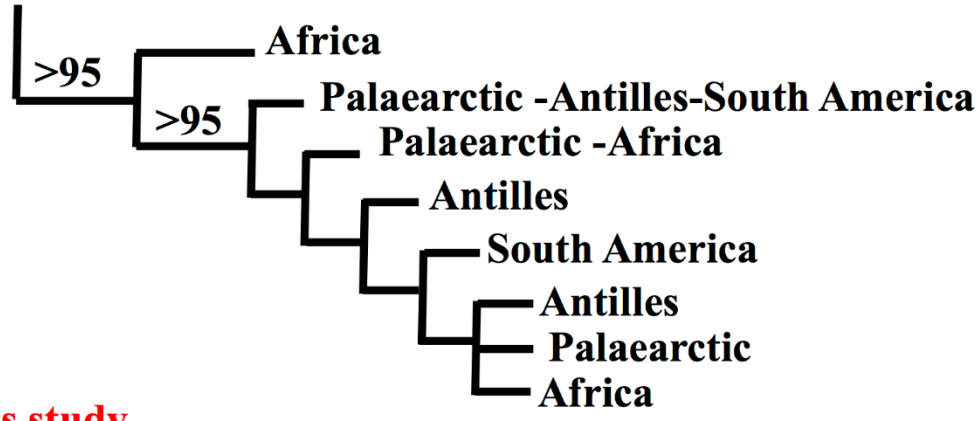

c) This study

Turdus philomelos **(Palaearctic)**

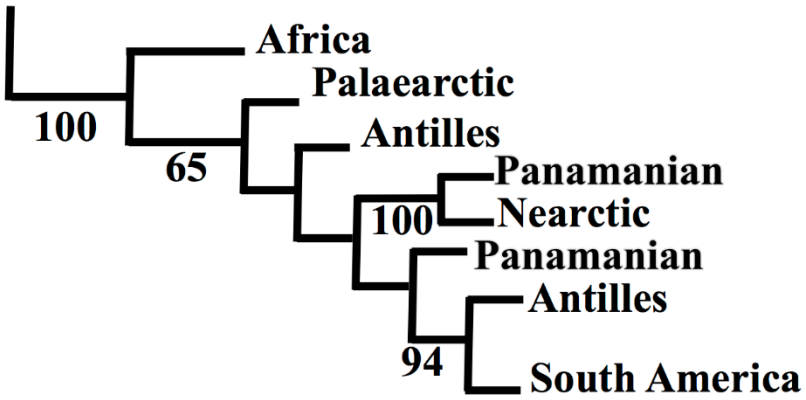

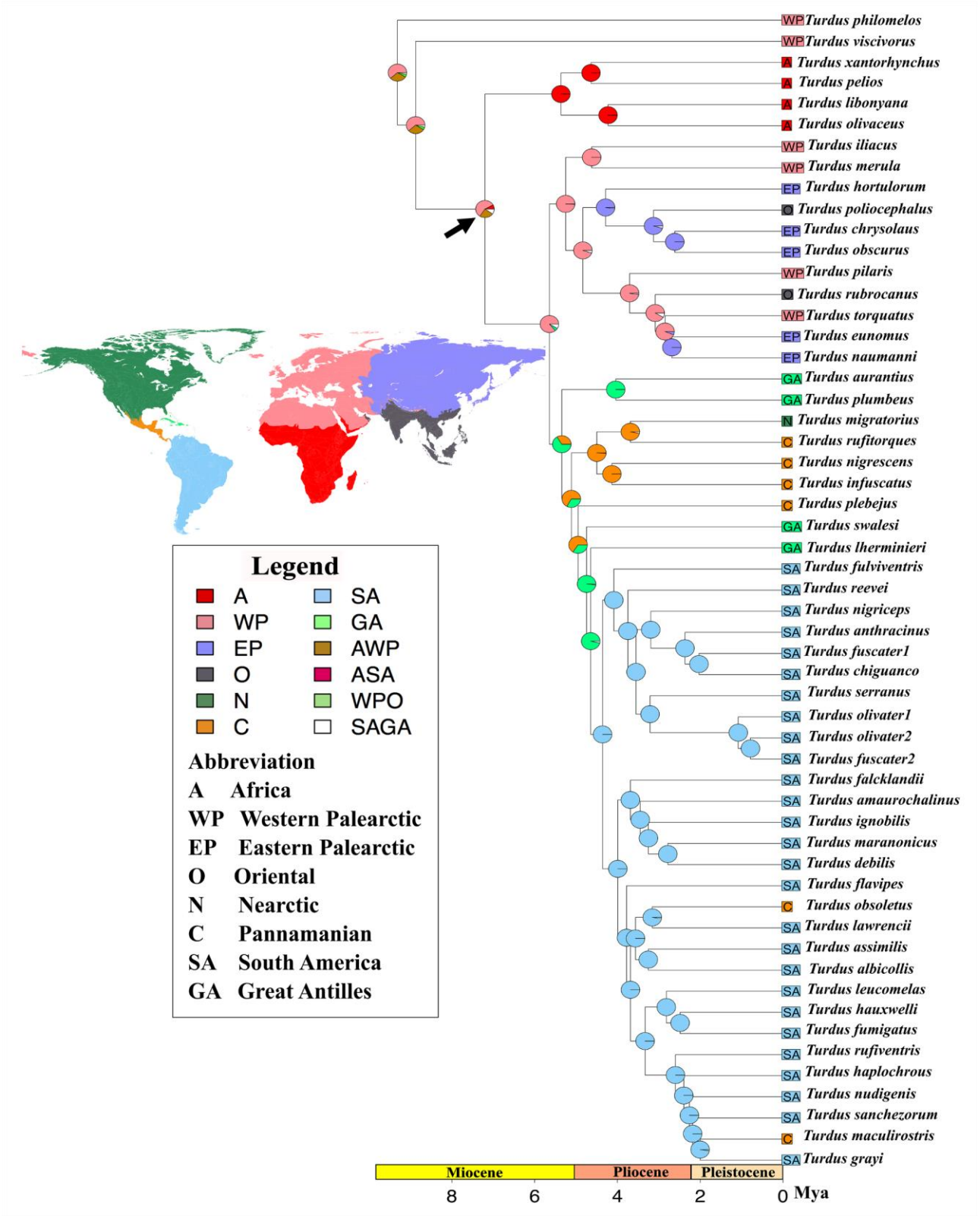
WP Turdus philomelos
WP Turdus viscivorus
A Turdus xantorhynchus
A Turdus pelios
A Turdus libonyana
A Turdus olivaceus
WP Turdus iliacus
WP Turdus merula
EP Turdus hortulorum
O Turdus poliocephalus
EP Turdus chrysolaus
EP Turdus obscurus
WP Turdus pilaris
O Turdus rubrocanus
WP Turdus torquatus
EP Turdus eunomus
EP Turdus naumanni
GA Turdus aurantius
GA Turdus plumbeus
N Turdus migratorius
C Turdus rufitorques
C Turdus nigrescens
C Turdus infuscatus
C Turdus plebejus
GA Turdus swalesi
GA Turdus lherminieri
SA Turdus fulviventris
SA Turdus reevei
SA Turdus nigriceps
SA Turdus anthracinus
SA Turdus fuscater1
SA Turdus chiguanco
SA Turdus serranus
SA Turdus olivater1
SA Turdus olivater2
SA Turdus fuscater2
SA Turdus falcklandii
SA Turdus amaurochalinus
SA Turdus ignobilis
SA Turdus maranonicus
SA Turdus debilis
SA Turdus flavipes
C Turdus obsoletus
SA Turdus lawrencii
SA Turdus assimilis
SA Turdus albicollis
SA Turdus leucomelas
SA Turdus hauxwelli
SA Turdus fumigatus
SA Turdus rufiventris
SA Turdus haplochrous
SA Turdus nudigenis
SA Turdus sanchezorum
C Turdus maculirostris
SA Turdus grayi
Legend
A
WP
EP
O
N
C
SA
GA
AWP
ASA
WPO
SAGA
Abbreviation
A Africa
WP Western Palearctic
EP Eastern Palearctic
O Oriental
N Nearctic
C Pannamanian
SA South America
GA Great Antilles
Miocene
Pliocene
Pleistocene
8
6
4
2
0 Mya